CHAPTER 5:

BCL11 GENES ARE ESSENTIAL FOR NORMAL MAMMARY DEVELOPMENT

5.1 Introduction

5.1.1 Genetic control of lymphocyte and mammary development

Gene regulatory networks are essential to the developmental process, orchestrating the process through a series of co-ordinated hierarchical stages, enabling the specification, commitment and differentiation of different cell fates from multi-potent stem or progenitor cells. Transcription factors play intricate roles in the gene regulatory networks which are made up of complementary sets of transcription activators and repressors that play antagonistic roles by activating the transcription of effector genes of a given cell fate while repressing that of alternate cell fates (Singh et al., 2005). Therefore homeostasis of the levels and modifications of transcription factors at various checkpoints during the developmental process is critical for the specification and maintenance of a certain cell fate. The initial specification of cell fate arises in part through juxtacrine and paracrine signalling pathways, such as Wnt and Notch that activate the initial node in the regulatory network (Singh et al., 2005). These transcription factors then auto-regulate in positive- or negative-feedback loops and activate or repress other members in a hierarchical fashion in order to establish the differentiated state. Each cell fate is therefore specified by a unique combination of transcription factors; the level and activity of each contribute to the specification and differentiation of the cell.

With the well-defined molecular markers for various stem/progenitor and differentiated cells, together with a well-established transplantation protocol in the mouse, the hematopoietic system is currently the most comprehensively understood stem cell developmental system. A combination of reverse genetics by loss-of-function analyses with knockout mouse models and forward genetic screens with retroviral integrations that resulted in development of leukaemia have uncovered transcription factors that are critical for the control of different hematopoietic lineages (Cantor and Orkin, 2001; Orkin and Zon, 2008). The Gata family of transcription factors are crucial

players in the gene regulatory networks that control the specification of cell fates (Ho and Pai, 2007; Kaufman et al., 2003; Kouros-Mehr et al., 2008). In particular, Gata-1 and Gata-3 are involved in the specification of hematopoietic cell fates. While Gata-1 is involved in erythropoeisis, Gata-3 is required for T-cell specification and T_H2 differentiation. In these hematopoietic lineages, Gata transcription factors on one hand promote the fate of a specific cell lineage, and on the other hand repress alternate lineages. For example, in T-helper cells, Gata-3 and T-bet exhibit transcriptional cross-antagonism which help the bi-potent progenitors to commit to one fate and also reinforce the specification and maintenance of T_H2 and T_H1 cell fates, respectively (Ho and Pai, 2007; Zheng and Flavell, 1997).

Research on mammary gland development in the mouse has been focused on steroid and peptide hormones and the contribution of their signalling pathways on mammary gland differentiation (Chapter 1.4.2-3) (Hennighausen and Robinson, 2005). Recent studies have identified several transcription factors that normally functions in lineage commitment in lymphocyte development, also play essential roles in mammary lineage commitment (Asselin-Labat et al., 2007; Khaled et al., 2007; Kouros-Mehr et al., 2006). Using mammary-specific transgenic Cre lines, *Gata-3* was conditionally deleted at various stages of mammary development and shown to be essential for the differentiation and maintenance of luminal cell fate (Asselin-Labat et al., 2007; Kouros-Mehr et al., 2006). Prolactin signalling is essential for the proliferation and functional differentiation of lobulo-alveolar structures during pregnancy (Topper and Freeman, 1980). The effects of prolactin signalling during pregnancy are predominantly mediated via Stat5 as discussed in Chapter 1.4.3.3-4. Recently, Stat6 and its upstream cytokines, IL4 and IL13, have also been shown to be required for luminal epithelial cell development (Khaled et al., 2007). In the *Stat6*$^{-/-}$ and *Il4*$^{-/-}$/*Il13*$^{-/-}$ double mutant mice, a 70% reduction in the number of alveoli was observed in the day 5 gestation gland, whereas deletion of *Socs5*, a negative regulator of Stat6, resulted in precocious alveolar development (Khaled et al., 2007). Taken together, these results suggest that genetic control of cell fate determination in mammary and lymphocyte lineages is highly parallel.

Bcl11a and *Bcl11b* are essential in lymphoid lineage specification as discussed in Chapter 1.3.4. These observations, together with the fact that two *BCL11A* mutations

were identified in human breast cancer (Wood et al., 2007), prompted me to investigate the functions of *Bcl11a* and *Bcl11b* in the mammary gland.

5.1.2 Clues from expression patterns

As discussed in Chapter 4, *Bcl11a* and *Bcl11b* exhibited unique and differential expression patterns in the mammary gland. Expression of both genes in the mammary lineages was detected in early embryonic development. In the virgin gland, *Bcl11a* was expressed in TEBs and in both luminal and basal cells while *Bcl11b* was expressed predominantly in the basal layer. Further analysis showed that *Bcl11a* was expressed in differentiated luminal and luminal progenitor cells. *Bcl11b* on the other hand, was expressed in only a small number of $Sca1^-$ ($ER\alpha^-$) luminal progenitors. Up-regulation of both genes was detected early in gestation; while expression of *Bcl11a* was maintained throughout gestation and lactation, levels of *Bcl11b* declined steadily from gestation to lactation. In the gestation gland, expression of *Bcl11a* was detected in both ductal and differentiating lobulo-alveolar structures while expression of *Bcl11b* was restricted predominantly to the basal cells. During lactation, only *Bcl11a* was detected in differentiated luminal secretory lobulo-alveoli. Taken together, these expression data implicate *Bcl11* genes may play important but different roles in the mammary epithelium – while *Bcl11a* may be important for luminal cell differentiation and maintenance, *Bcl11b* may have a critical role in the basal cells.

In this Chapter, I will first describe the mammary phenotypes in the *Bcl11* homozygous mutant embryos. I will then discuss the mammary defects in the virgin gland of the *Bcl11* conditional knockout mice after deleting *Bcl11* genes.

5.2 Results

5.2.1 Loss of *Bcl11a* leads to abnormal mammary bud formation

To study the physiological role of *Bcl11a* and *Bcl11b* in embryonic development, heterozygous *Bcl11*$^{lacZ/+}$ breeding pairs were set up and female mice were subjected to timed pregnancies. Embryos were collected, staged and genotyped to identify the *Bcl11* homozygous mutant embryos for analysis.

Murine mammary development is evident at 10.5 day post-coitum (dpc) with the appearance of milk lines in the embryos (Veltmaat et al., 2004). At 11.5 dpc, the milk lines have developed into five pairs of mammary placodes that occupy specific positions along the ventral side of the embryo (Watson and Khaled, 2008). The placodes are formed asynchronously in a specific order. Several genes such as *Tbx3*, *Lef1*, *Fgf10* and *Fgfr2b* have been implicated in the formation of different placodes (Eblaghie et al., 2004; Mailleux et al., 2002; van Genderen et al., 1994).

I first analyzed the *Bcl11a*$^{lacZ/lacZ}$ homozygous mutant embryos. Expression of *Bcl11a* was detected in the mammary buds from 13.5 dpc. Anatomical examinations of *Bcl11a*$^{lacZ/lacZ}$ homozygous mutant embryos failed to identify the presence of mammary buds at 14.5 dpc. To determine the mammary phenotypes, *in situ* hybridization with *Fgfr2TK* antisense probe was performed. *Fgfr2TK* is expressed in the mammary primordial from 11.5 dpc (Mailleux et al., 2002) and *in situ* hybridization with this antisense probe showed that all five pairs of mammary buds were formed in the *Bcl11a*$^{lacZ/lacZ}$ homozygous mutant 13.5-14 dpc embryos (Figure 5.1A). However, all the mammary buds in the *Bcl11a*$^{lacZ/lacZ}$ homozygous mutant embryos had a flattened morphology whereas those in the wild-type embryos had a discrete lens-shaped structure (Figure 5.1A). *Notch1* is expressed specifically in the mammary buds during embryonic development (Personal communication with Christine Watson). Examination of wild-type and *Bcl11a*$^{lacZ/lacZ}$ homozygous mutant 13.5-14 dpc embryos using *Notch1* antisense probe showed that expression of *Notch1* was detected only in the fourth and fifth pair of mammary buds. Consistent with the results obtained using *Fgfr2TK* probe, *in situ* hybridization with *Notch1* antisense probe confirmed that the mammary buds in *Bcl11a*$^{lacZ/lacZ}$ homozygous mutant embryos had a less developed morphology as

compared to the wild-type embryos which formed large, round knob-shaped structures (Figure 5.1B).

Lef1 exhibits a dynamic expression pattern during embryonic mammary development (Foley et al., 2001). Between 11-12 dpc, *Lef1* is expressed in basal cells of developing epidermis and in epithelial cells of the mammary buds and from 13.5 dpc, expression of *Lef1* is induced within mesenchymal cells of the developing mammary buds as it is fading away in the mammary epithelium. By 14.5-15.5 dpc, in the epidermis destined to become nipple sheath, *Lef1* expression becomes undetectable. At 14.5 dpc, expression of *Lef1* was detected only in the epidermis of the fifth pair of mammary buds in the wild-type embryos. In contrast, *Lef1* expression was detected in all the epidermis of the mammary buds in $Bcl11a^{lacZ/lacZ}$ homozygous mutant embryos (Figure 5.1C).

In male embryos at 15.5 dpc, the epithelial buds became separated from the epidermis under the influence of testosterone resulting in active induction of apoptosis by the mammary mesenchyme (Wysolmerski et al., 1998). This resulted in the regression of mammary buds in male embryos and *in situ* hybridization with *Fgfr2TK* antisense probe revealed no mammary epithelial remnants in wild-type male embryos at 16.5 dpc (n=1) (Figure 5.1D1-3). In contrast, presence of rudimentary mammary buds in $Bcl11a^{lacZ/lacZ}$ homozygous mutant male embryos at 16.5 dpc was detected using *in situ* hybridization with antisense *Fgfr2TK* probe (n=1) (Figure 5.1D4-6), suggesting that loss of *Bcl11a* resulted in failure of regression of mammary buds. *Lef1* has been shown to be an important mesenchymal survival factor (Boras-Granic et al., 2006) as $Lef1^{-/-}$ embryos showed arrested development and subsequent regression in mammary placodes. Therefore, the continual expression of *Lef1* in the mammary buds (possibly in both epidermis and mesenchyme) of $Bcl11a^{lacZ/lacZ}$ homozygous mutant 14.5 dpc embryos might explain the presence of rudimentary mammary buds in the male embryo at 16.5 dpc. Taken together, loss of *Bcl11a* results in defective embryonic mammary formation and failure in regression of mammary epithelial in the male embryo.

A

13.5-14 dpc (*Fgfr2TK*)

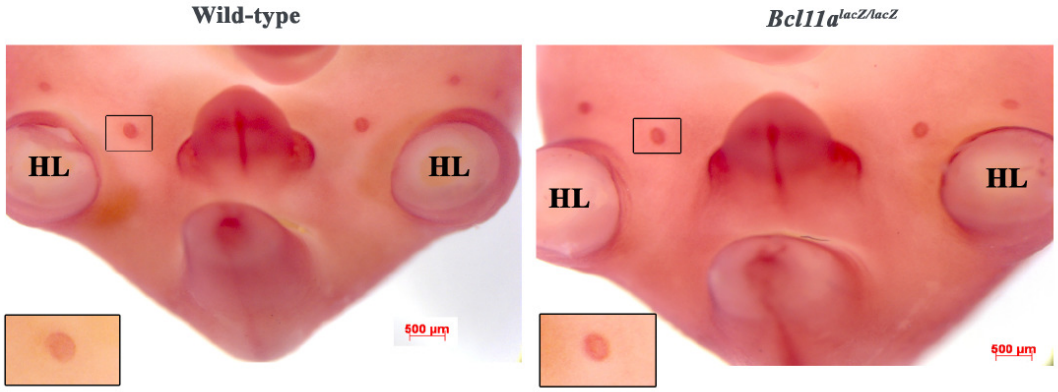

B

13.5-14 dpc (*Notch1*)

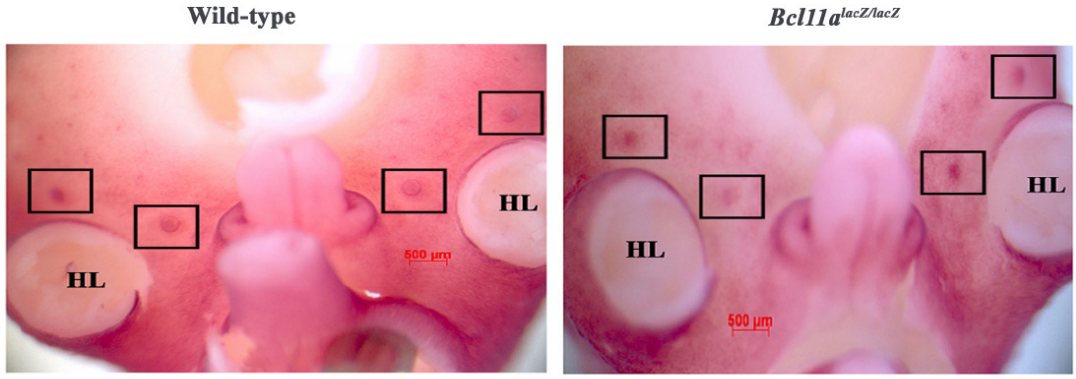

C

14.5 dpc (*Lef1*)

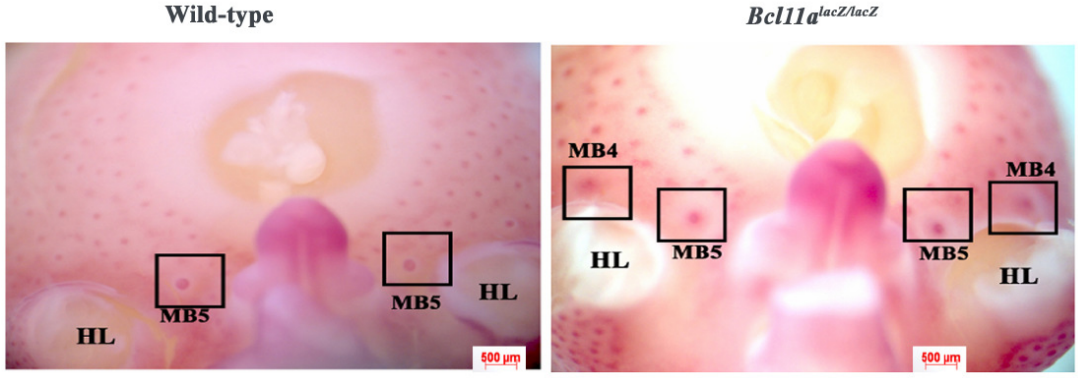

D

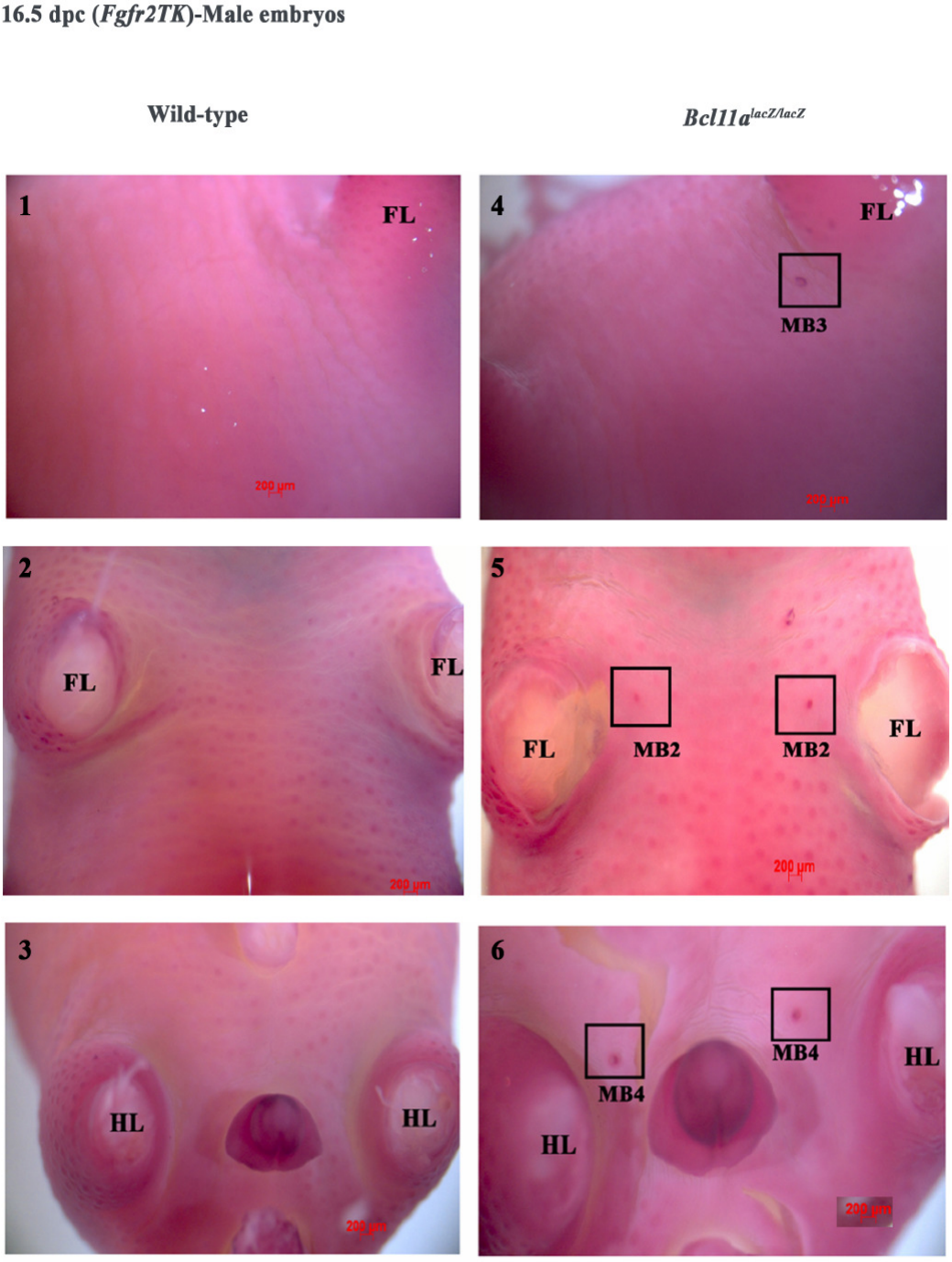

Figure 5.1. *In situ* hybridization of wild-type and *Bcl11a*$^{lacZ/lacZ}$ homozygous mutant embryos. Whole mount images of *in situ* hybridization of wild-type and *Bcl11a*$^{lacZ/lacZ}$ homozygous mutant 13.5-14 dpc embryos with **(A)** *Fgfr2TK*, **(B)** *Notch1* and **(C)** *Lef1* antisense probes. Inserts are higher magnification of mammary buds. Whole mount images of *in situ* hybridization of wild-type **(D1-3)** and *Bcl11a*$^{lacZ/lacZ}$ homozygous mutant **(D4-5)** 16.5 dpc male embryo with *Fgfr2TK* antisense probe. Boxed regions indicate presence of buds in *Bcl11a*$^{lacZ/lacZ}$ homozygous mutant male embryo. FL – Forelimb; HL – Hindlimb; MB – Mammary Bud.

5.2.2 *Bcl11b* is essential for formation of third pair of mammary buds

Bcl11b is expressed in all mammary placodes from 12.5 dpc. In the *Bcl11b*$^{lacZ/lacZ}$ homozygous mutant 12.5-13.5 dpc embryos, expression of *Bcl11b* was not detected in the third pair of mammary buds (Figure 5.2A). This suggests that the third pair of mammary buds may be missing in the *Bcl11b*$^{lacZ/lacZ}$ homozygous mutant embryos. To confirm the effects of loss of *Bcl11b* on mammary buds, whole mount *in situ* hybridization using *Wnt10b* was performed. *Wnt10b* is one of the earliest markers of the mammary epithelium and is expressed from 10.5 dpc, beginning as a diffuse line (milk line) that eventually breaks up into individual spots (mammary placodes) by 12.5 dpc (Veltmaat et al., 2004). As shown in Figure 5.2B, expression of *Wnt10b* was abolished in the third pair of mammary placodes and also greatly reduced in the second and fourth pairs of mammary placodes in the *Bcl11b*$^{lacZ/lacZ}$ homozygous mutant 12.5 dpc embryos. This established that *Bcl11b* is essential for the formation of the third pair of mammary buds. This mammary defect was further confirmed by *in situ* hybridization with the antisense *Lef1* and *Fgfr2TK* probes. Similar to *Wnt10b*, expression of *Lef1* was absent in the third pair and reduced in the other pairs of mammary buds of the *Bcl11b*$^{lacZ/lacZ}$ homozygous mutant 12.5 dpc embryos (Figure 5.2C). In later stage embryos (14.5 dpc), expression of *Fgfr2TK* was not detected in the third pair and was greatly reduced in other pairs of mammary buds of the *Bcl11b*$^{lacZ/lacZ}$ homozygous mutant embryos (Figure 5.2D). These results confirmed that in the absence of *Bcl11b*, formation of the third pair of mammary buds was completely abolished while formation of other mammary buds was also affected.

To further dissect the mammary development defects in *Bcl11b*$^{lacZ/lacZ}$ homozygous mutant embryos, *in situ* hybridization on younger embryos (10.5 dpc) using other markers was performed. *Fgf10* expression is first detected in the presumptive mammary region at 10.5 dpc and its expression extends as a line from the forelimb bud to the level of somite 18 (where the third pair of mammary buds will subsequently form) in the dermamyotome (Mailleux et al., 2002). *Tbx3* expression is also observed as a thin line marking what appears to be the mammary line from 10.25 dpc (Eblaghie et al., 2004). Graded *Tbx3* expression is also observed with highest levels of transcripts present

adjacent to the posterior margin of the forelimb bud and gradually diminishing down the flank to the anterior limit of the hindlimb bud. *Tbx3* expression at 10.5 dpc is stronger than at 10.25 dpc and from 11.5 dpc, expression of *Tbx3* is observed in the mammary placodes. *Fgf10* and *Tbx3* expression patterns were similar in *Bcl11b*$^{lacZ/lacZ}$ homozygous mutant and wild-type embryos at 10.5 dpc, prior to mammary bud formation (Figure 5.2E-F). Expression of *Fgf10* in the lateral plate mesoderm was detected in both wild-type and *Bcl11b*$^{lacZ/lacZ}$ homozygous mutant 10.5 dpc embryos as a line extending from the forelimb bud to the level of the future site of the third pair of mammary placodes (Figure 5.2E). Similarly, expression of *Tbx3* was observed in the presumptive milk line in both wild-type and *Bcl11b*$^{lacZ/lacZ}$ homozygous mutant 10.5 dpc embryos (Figure 5.2F). These results indicated that expression of mesodermal mammary line markers, *Fgf10* and *Tbx3*, were unaffected in the *Bcl11b*$^{lacZ/lacZ}$ homozygous mutant embryos, suggesting that specification of the mammary line was unaltered. A similar phenotype was observed in the *ska* homozygous mice where the gene affected in *ska* mice was mapped to Neuregulin3 (*Nrg3*) (Howard et al., 2005). In these mice, the third pair of mammary bud is hypoplastic from 11.75 dpc, leading to a reduced sized or absent bud. It has been suggested that *Nrg3* could act to transmit signals from *Fgf10* and/or *Tbx3* to the precursor mammary epithelial cells which appear to express *Wnt10b* (Veltmaat et al., 2004). Taken together, my results suggest that *Bcl11b* may function downstream of *Fgf10* and *Tbx3* but upstream of *Wnt10b* and *Lef1* in the specification and/or formation of number 3 pair of mammary buds and may function in concert with *Nrg3* to transmit signals from *Fgf10* and/or *Tbx3* to the precursor mammary epithelial cells. Alternatively, *Bcl11b* may also function in an alternative pathway for the formation of the third pair of mammary buds. Collectively, these results demonstrate the importance of both *Bcl11a* and *Bcl11b* in embryonic mammary development.

A

(Whole mount X-gal)

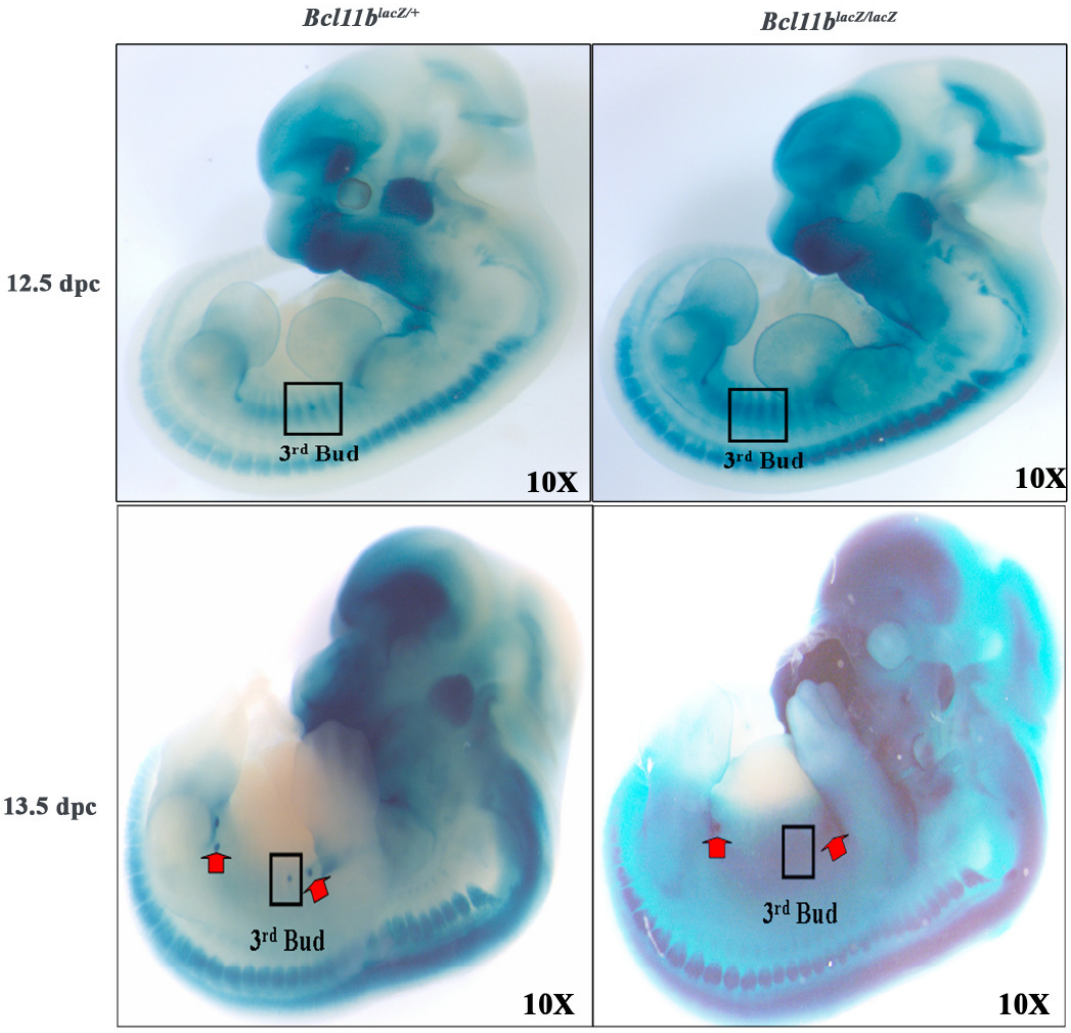

B 12.5 dpc (*Wnt10b*)

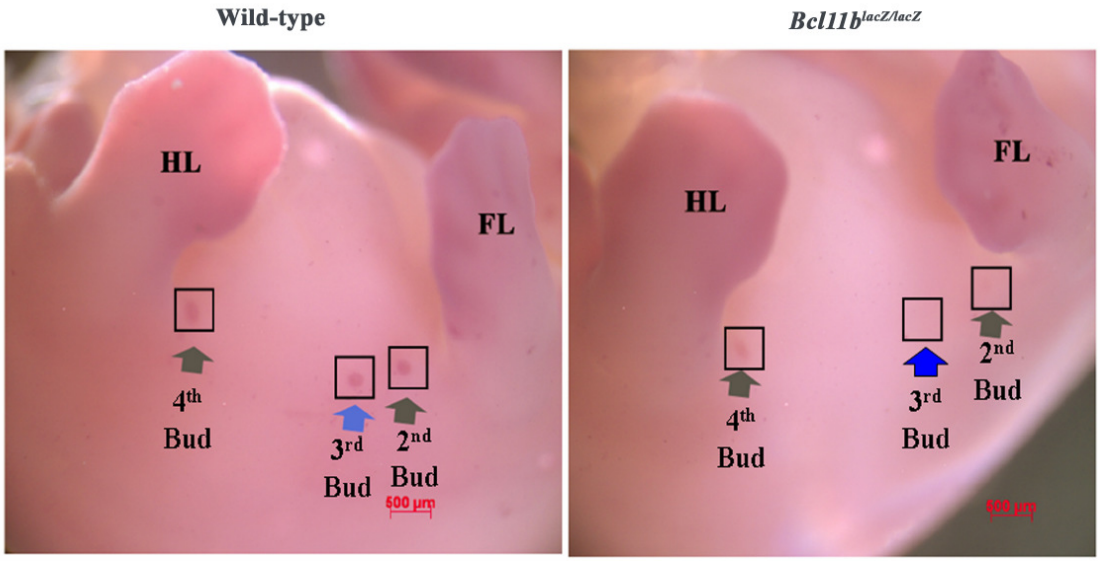

C 12.5 dpc (*Lef1*)

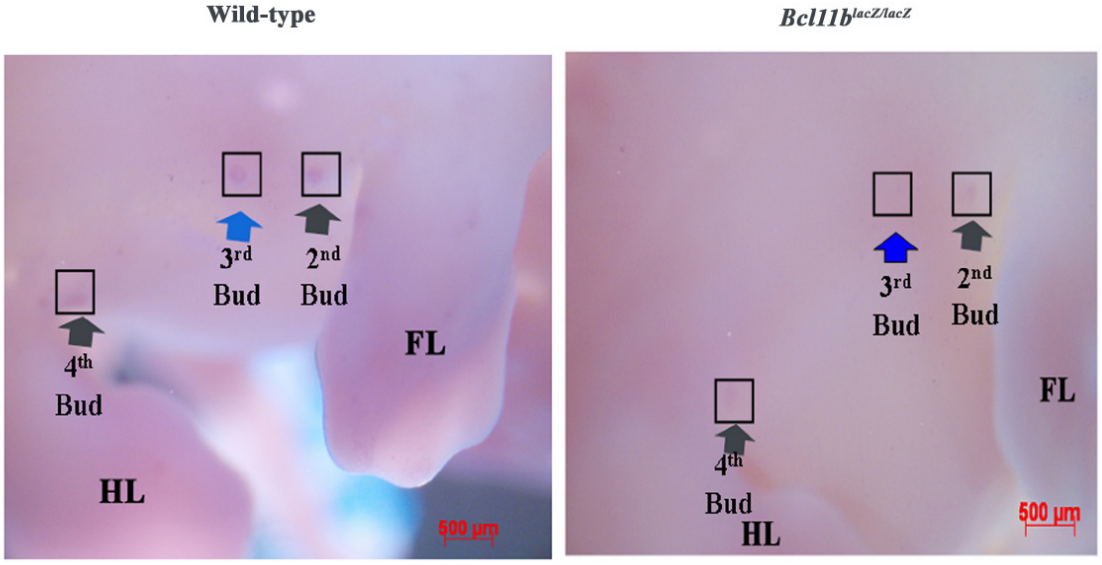

D

14.5 dpc (*Fgfr2TK*)

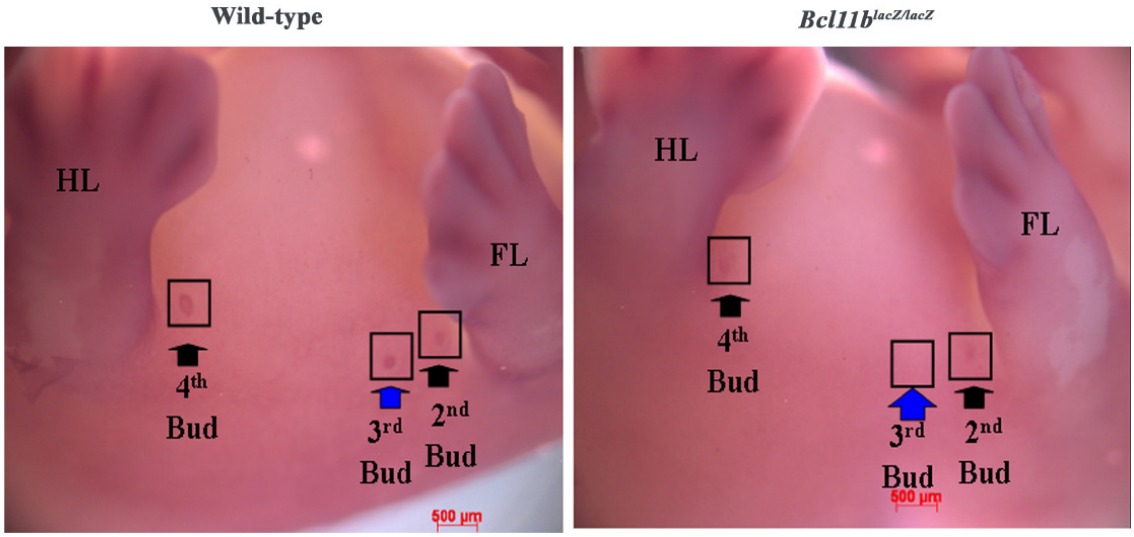

E

10.5 dpc (*Fgf10*)

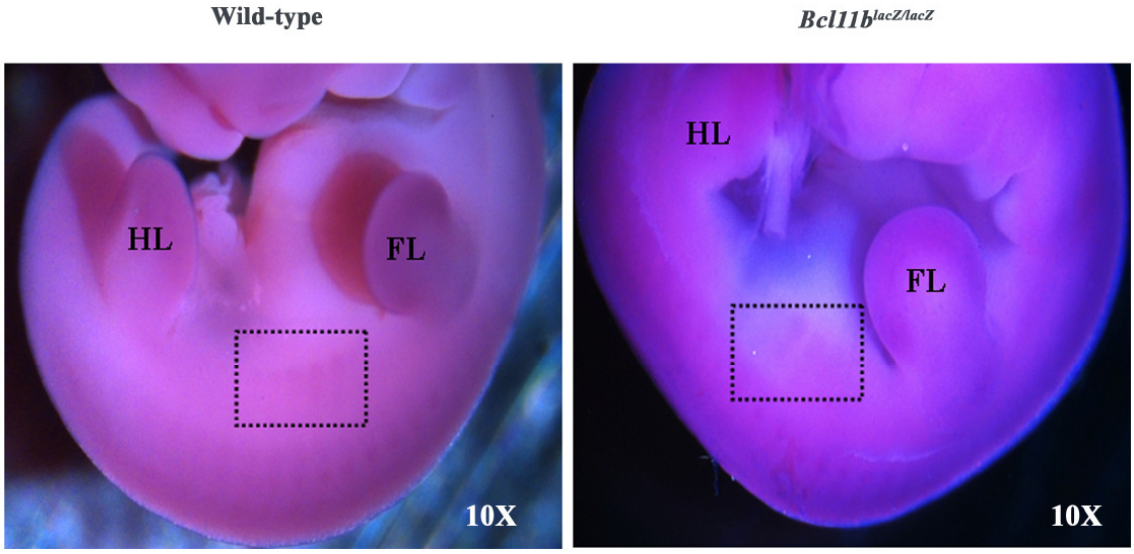

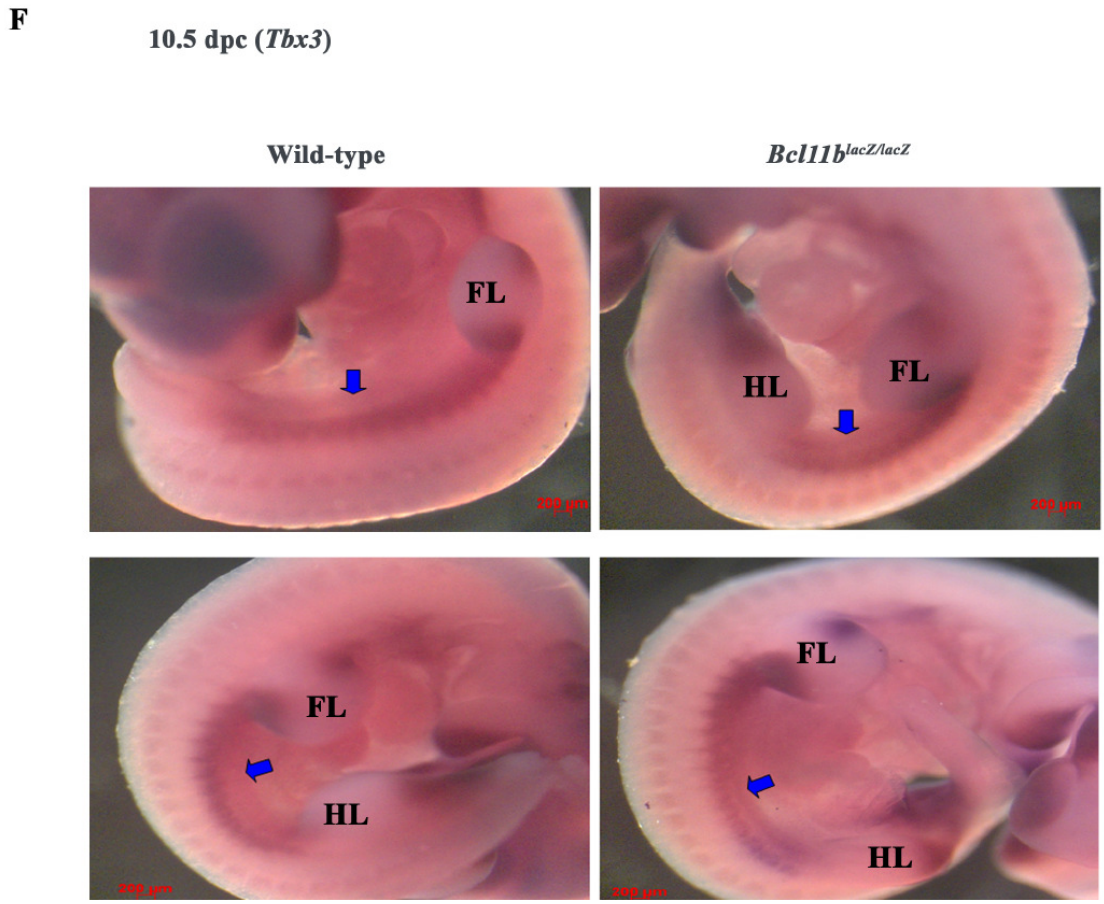

Figure 5.2. Analysis of *Bcl11b*$^{lacZ/lacZ}$ homozygous mutant embryos using X-gal staining and *in situ* hybridization. **(A)** Whole mount images of X-gal staining of *Bcl11b*$^{lacZ/+}$ heterozygous and *Bcl11b*$^{lacZ/lacZ}$ homozygous mutant 12.5 dpc and 13.5 dpc embryos. Boxed regions show the approximate position of the third mammary bud. Red arrows indicate position of the second and fourth mammary buds. **(B-D)** Whole mount images of *in situ* hybridization of wild-type and *Bcl11b*$^{lacZ/lacZ}$ homozygous mutant 12.5 dpc embryos with **(B)** *Wnt10b* and **(C)** *Lef1* antisense probes; wild-type and *Bcl11b*$^{lacZ/lacZ}$ homozygous mutant 14.5 dpc embryos with **(D)** *Fgfr2TK* antisense probe. Boxed regions with black arrows show position of the second and fourth pairs of mammary buds while boxed regions with blue arrows show position of the third pair of mammary buds. Whole mount images of *in situ* hybridization of wild-type and *Bcl11b*$^{lacZ/lacZ}$ homozygous mutant 10.5 dpc embryos with **(E)** *Fgf10* and **(F)** *Tbx3* antisense probes. Boxed region shows the region of positive Fgf10 staining. Blue arrows show the location of the presumed milk line as indicated by Tbx3 staining in the embryos. FL – Forelimb; HL – Hindlimb.

5.2.3 Loss of *Bcl11a* in virgin glands causes disruption of mammary architecture

Both *Bcl11* null mice died several hours after birth from unknown reasons (Liu et al., 2003b; Wakabayashi et al., 2003b), so I was unable to use these mice to study postnatal mammary development. Therefore, our lab utilized recombineering to generate conditional knockout (cko) alleles of both *Bcl11* genes ($Bcl11^{flox/flox}$) (Mice were generated by Pentao Liu). In the cko mice, exon 1 and exon 4 of *Bcl11a* and *Bcl11b* were flanked by *lox*P sites respectively (Figure 5.3A-D); upon expression of Cre recombinase, the intervening sequences between the *lox*P sites will be deleted, resulting in inactivation of the genes. These cko mice were subsequently crossed to several Cre-lines to delete *Bcl11* genes temporally and spatially in the mammary gland.

To examine whether *Bcl11a* and *Bcl11b* are required for mammary development in the virgin gland, I first crossed the $Bcl11^{flox/flox}$ mice to the Rosa26-CreERT2 mice where *Cre-ERT2* fusion gene expression is controlled by the constitutive active *Rosa26* promoter (Hameyer et al., 2007). In the CreERT2 protein, Cre is fused to the ligand-binding domain of a mutated human estrogen receptor (ERT) that recognizes tamoxifen (TAM) or its derivative 4-hydroxytamoxifen (4-OHT). Homozygous floxed mice carrying the *Rosa26-CreERT2* allele (*CreERT2;* $Bcl11a^{flox/flox}$) were born in a normal Mendelian ratio. The females of the *CreERT2;* $Bcl11^{flox/flox}$ mice were able to nurse and nurture their pups. Whole mount and histological analyses of mammary glands from *CreERT2;* $Bcl11^{flox/flox}$ females appeared normal with no noticeable developmental defects. To gain insight into the function of *Bcl11a* in the virgin mammary gland, TAM was administrated to 4-8-week-old *CreERT2;* $Bcl11a^{flox/flox}$ and control (*CreERT2;* $Bcl11a^{flox/+}$ heterozygous and wild-type) females to induce *Bcl11a* deletion. The injected mice were analyzed three weeks post injection. Genomic DNA was extracted from TAM-injected mammary glands and Cre-mediated excision was detected using PCR primers as shown in Figure 5.4A. Cre-mediated excision of *Bcl11a* was confirmed by the presence of deletion bands in the mammary glands (Figure 5.4B) and quantitative real time PCR (qRT-PCR) amplification of genomic DNA derived from these mammary glands showed that the deletion efficiency was ~60%.

Whole-mount analysis of the mammary glands of control females did not reveal any obvious defects following TAM administration (Figure 5.5A). In contrast, the mammary glands of *CreERT2; Bcl11a*$^{flox/flox}$ homozygous females had enlarged primary ducts and reduced secondary and tertiary branches as compared to control glands (Figure 5.5A). Histological examination demonstrated that lumens of the mammary ducts were distended and lined by a thin epithelium with no clear distinction between the luminal and basal/myoepithelial layers as compared to the control glands (Figure 5.5B). The ducts appeared to have a thin cell layer in many areas instead of the distinct luminal and basal layers in the control ducts. To determine if basal and luminal cells were still present in this thin layer of epithelium cells, immunohistochemistry was conducted using antibodies to luminal marker Aquaporin 5 (Shillingford et al., 2003) and basal marker, cytokeratin 14 (CK14). The dilated ducts were stained positively for both markers, indicating that some luminal and basal epithelial cells were still present (Figure 5.6A). The disruption in mammary architecture was exemplified by the Aquaporin 5 positive luminal layer and CK14 positive basal layer forming a thin epithelial layer in the *Bcl11a*-deficient mammary glands (Figure 5.6A). This was confirmed by using additional basal markers such as p63 and smooth muscle actin (SMA), and luminal marker, cytokeratin 18 (CK18) (Figure 5.6B-D). Interestingly, some regions of the epithelium in *Bcl11a*-deficient glands appeared to be monolayered with basal and luminal cells found within the same layer (Figure 5.6A-D). Next, to determine whether deletion of *Bcl11a* led to abnormal proliferation or cell death, the mammary sections were stained with antibodies to cleaved Caspase 3 and Ki67. No obvious differences between the mutant and the control glands were observed, though a slight decrease in the number of Ki67 positive cells was observed in the mutant (Figure 5.7A and 5.7B). This suggests that loss of *Bcl11a* did not result in abnormal proliferation and apoptosis of mammary epithelial cells in the virgin glands. Alternatively, this may also suggest that the proliferative and apoptotic abnormalities occurred shortly after TAM injection and were thus not detected at the time of analysis (3 weeks after injection).

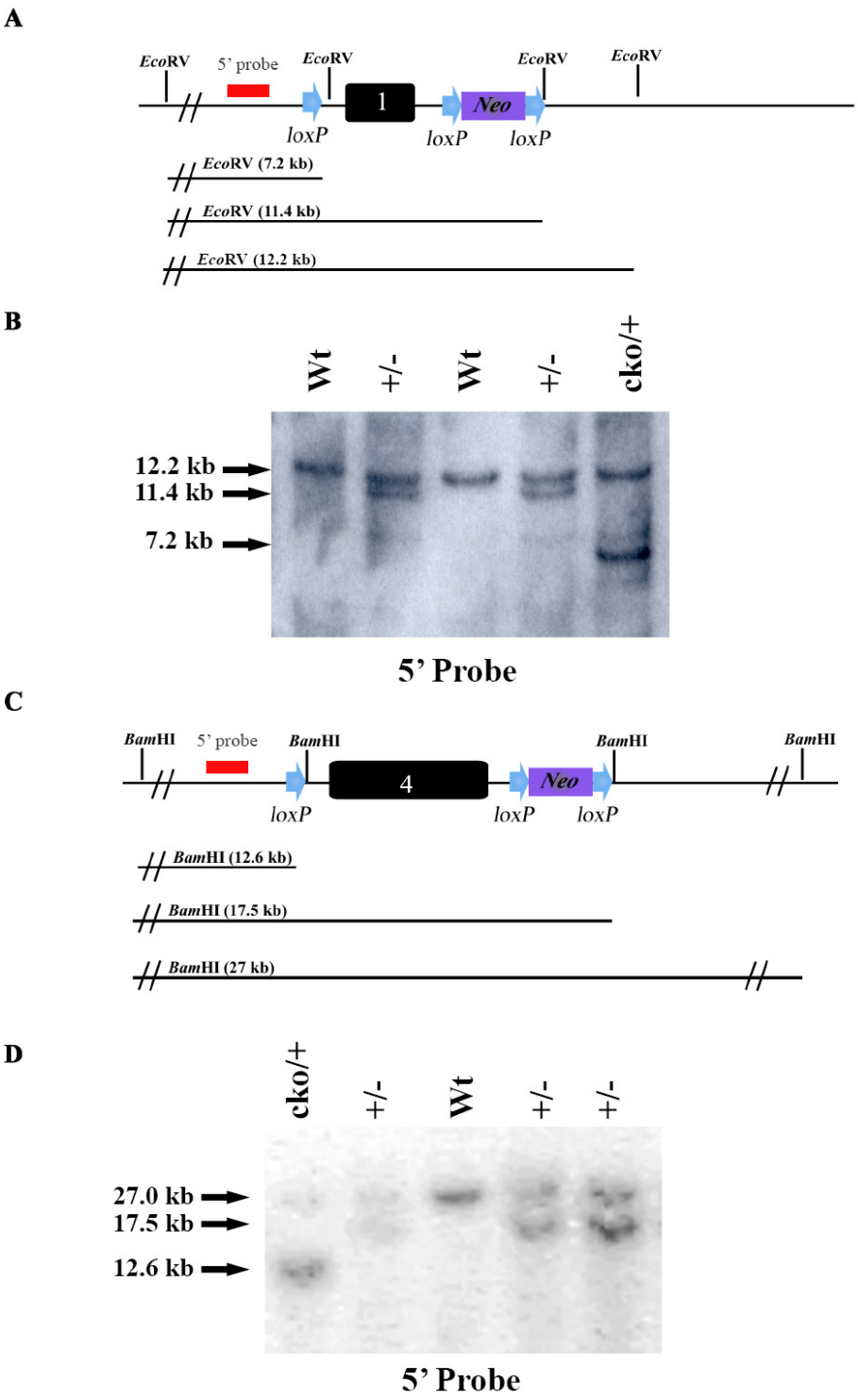

Figure 5.3. Generation of the *Bcl11* conditional knockout mice. **(A)** Schematic diagram showing targeting strategy of the *Bcl11a* conditional knockout (cko) allele. **(B)** Southern blot confirmation of the *Bcl11a* cko allele using 5' probe. Presence of cko allele is detected by a 7.2 kb band in the Southern analysis. **(C)** Schematic diagram showing targeting strategy of the *Bcl11b* cko allele. **(D)** Southern blot confirmation of the *Bcl11b* cko allele using 5' probe. Presence of cko allele is detected by a 12.6 kb band in the Southern analysis. (Southern blot analysis data provided by Pentao Liu).

A

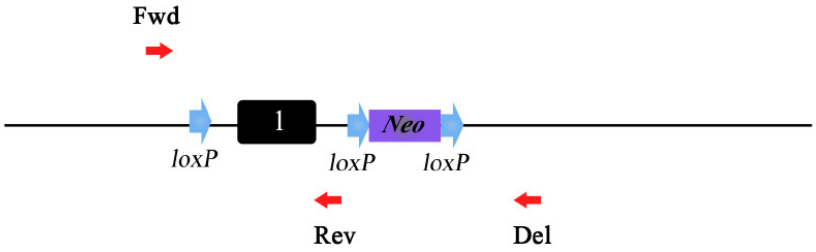

Fwd x Rev = 470 bp (Cko band)
Fwd x Del = 700 bp (Deletion band)

B

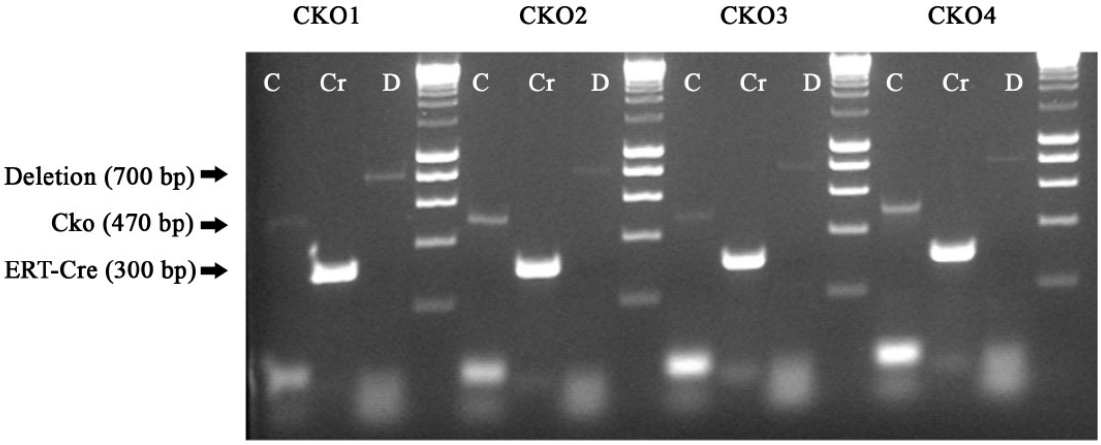

Figure 5.4. Detection of deletion of *Bcl11a* after Cre expression. **(A)** Schematic diagram showing relative position of primers in the *Bcl11a* locus used for detection of deletion band after Cre expression. **(B)** Gel image showing PCR products obtained with primers using genomic DNA extracted from mammary glands of tamoxifen injected *Cre-ERT2; Bcl11a*$^{flox/flox}$ mice. CKO1-4 represents mammary glands from four independent mice. C: cko PCR; Cr: Cre PCR; D: Deletion PCR.

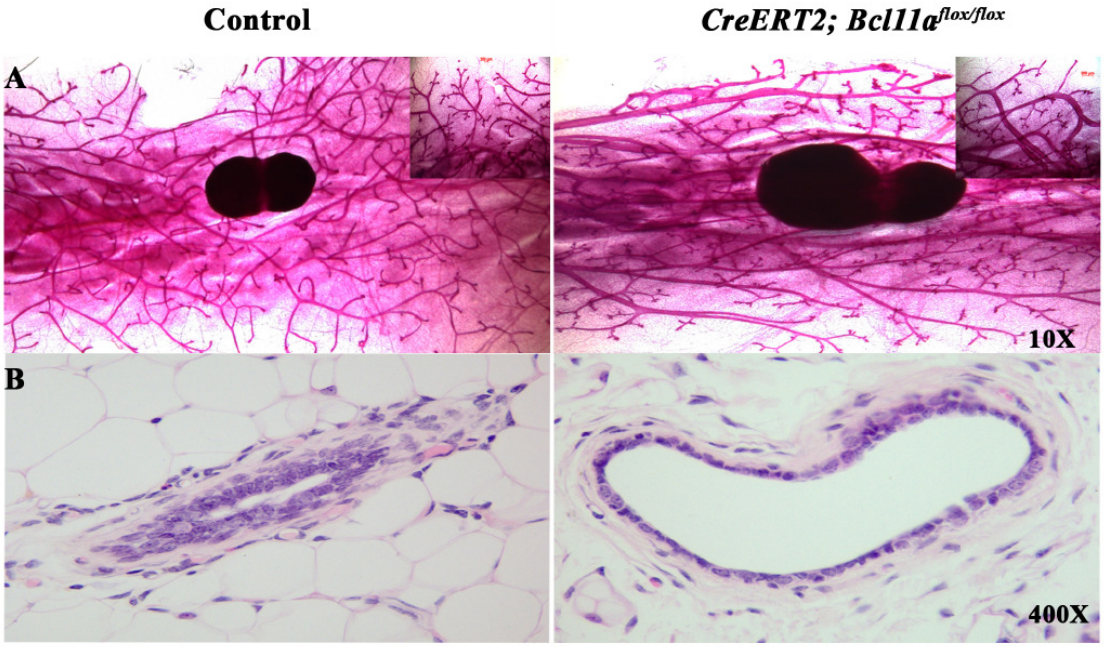

Figure 5.5. Morphological analysis of tamoxifen treated control and *Cre-ERT2; Bcl11a*$^{flox/flox}$ mammary glands. (A) Whole mount carmine alum-stained and **(B)** H&E stained sections of TAM injected control (Wild-type/*CreERT2*; *Bcl11a*$^{flox/+}$) and *CreERT2*; *Bcl11a*$^{flox/flox}$ mammary glands.

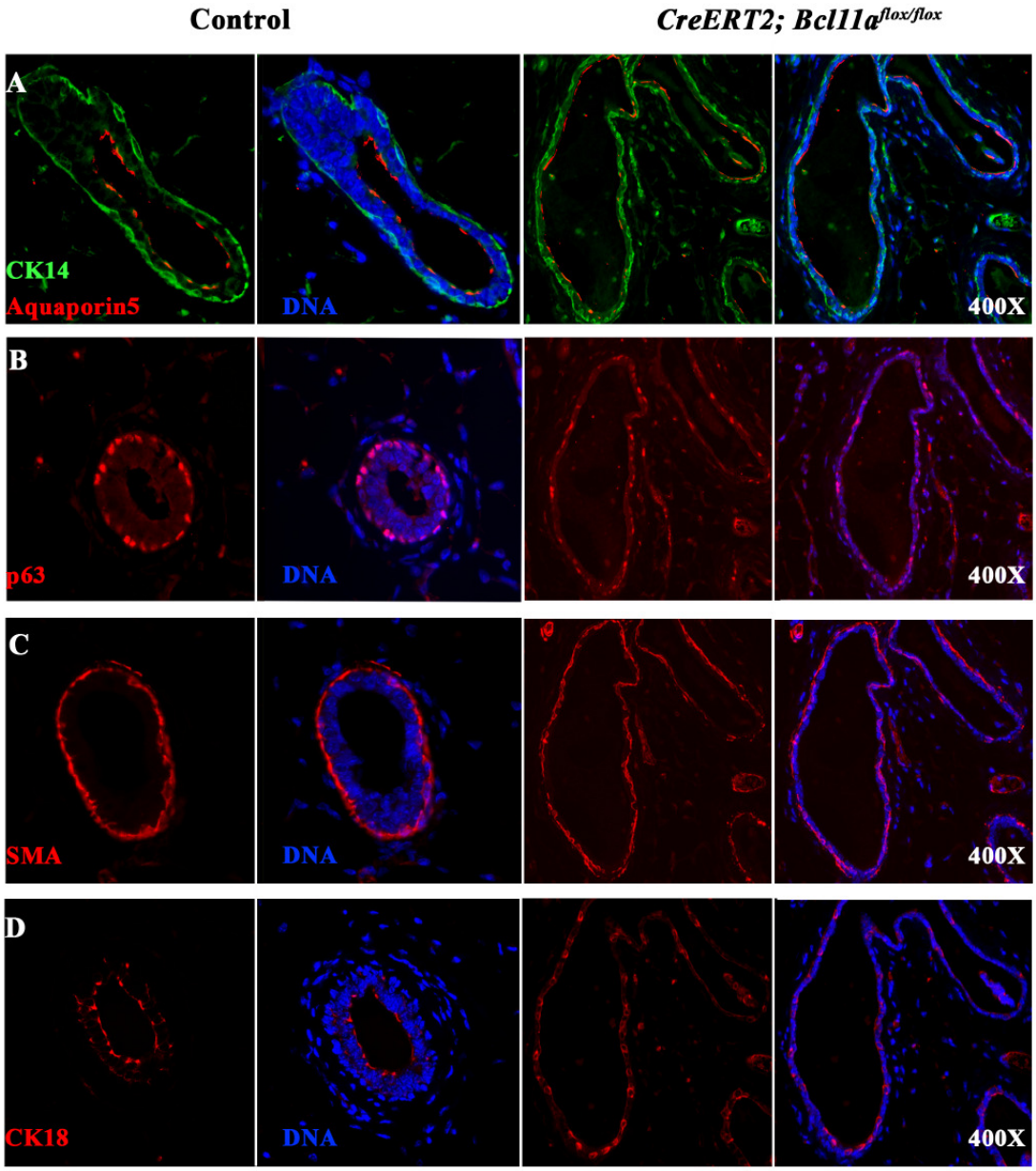

Figure 5.6. Immunohistochemical analysis of tamoxifen treated control and *Cre-ERT2; Bcl11a*$^{flox/flox}$ mammary glands sections using luminal/basal markers. Immunostaining of sections using antibodies against **(A)** Aquaporin 5, CK14, **(B)** p63, **(C)** SMA and **(D)** CK18. Control: Wild-type/*CreERT2*; *Bcl11a*$^{flox/+}$.

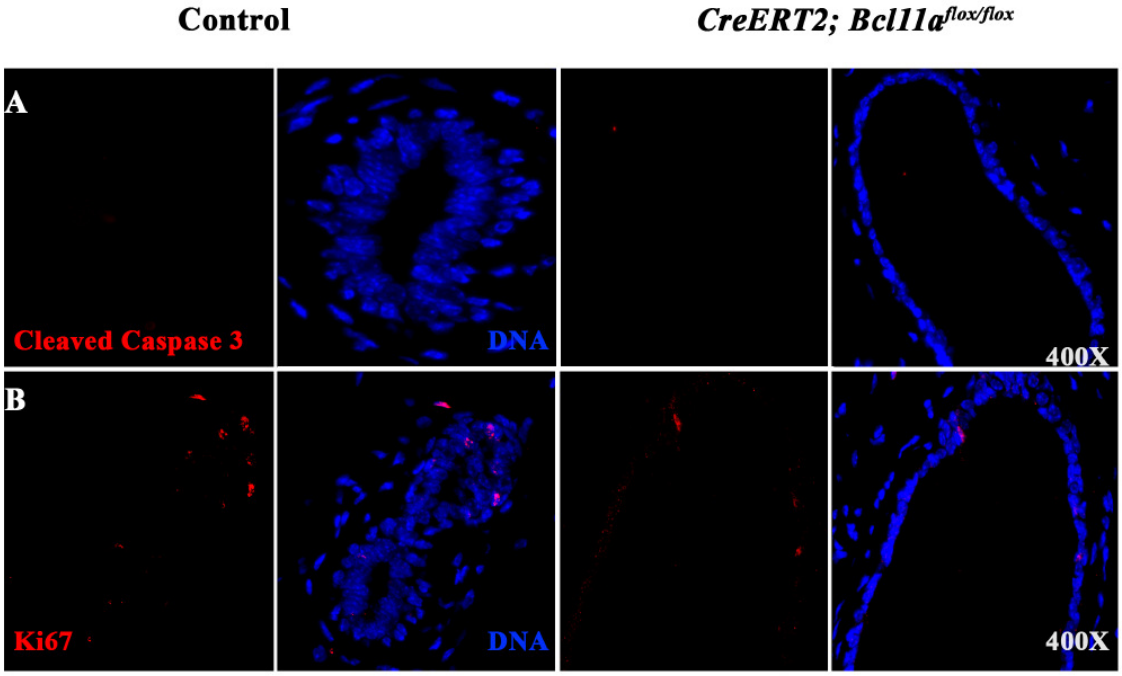

Figure 5.7. Immunohistochemical analysis of tamoxifen treated control and *Cre-ERT2; Bcl11a*$^{flox/flox}$ mammary glands. Immunostaining of sections using antibodies against **(A)** Cleaved Caspase 3 and **(B)** Ki67. Control: Wild-type/*CreERT2*; *Bcl11a*$^{flox/+}$.

5.2.4 Loss of *Bcl11a* in the mammary epithelium results in a loss of Gata-3$^+$ and an increase in ERα$^+$ epithelial cells

Gata-3 is the most highly enriched transcription factor in the mammary ductal epithelium and has recently been shown to be essential for the maintenance of luminal cell fate (Asselin-Labat et al., 2007; Kouros-Mehr et al., 2006). Interestingly, I found that loss of *Bcl11a* in the virgin glands resulted in a dramatic reduction in the number of Gata-3$^+$ luminal cells, suggesting a general loss of luminal cells (Figure 5.8A).

Estrogen receptor (ER) is required for ductal proliferation and differentiation (Korach, 2000). In the wild-type virgin gland, up to 37% of the luminal cells in the ducts and alveoli are ERα-positive (ERα$^+$), and most of these ERα$^+$ cells seem to be non-dividing cells that instruct adjacent epithelial cells to proliferate via paracrine regulatory effects (Clarke et al., 1997; Mallepell et al., 2006; Russo et al., 1999; Seagroves et al., 1998). It has been shown that the basal mammary stem cell (MaSC)-enriched population is ERα and progesterone receptor (PR) negative, and that ERα is localized to the more differentiated luminal cells (Asselin-Labat et al., 2006; Asselin-Labat et al., 2007; Lindeman and Visvader, 2006). The luminal population is composed of two phenotypically distinct lineages (Stingl and Watson, manuscript in preparation) (Sleeman et al., 2007). The Sca1$^+$ lineage is characterized by high levels of ERα expression whereas the Sca1$^-$ lineage is characterized by high levels of milk proteins expression. Hence, the Sca1$^+$ luminal progenitors were hypothesized to give rise to ERα$^+$ differentiated cells whereas the Sca1$^-$ luminal progenitors to function as alveolar precursors (Personal communication with John Stingl). Since *Bcl11a* is expressed in both the Sca1$^+$ and the Sca1$^-$ luminal progenitors, I examined the ERα status in the *Bcl11a*-deficient virgin glands. In the *Bcl11a*-deficient virgin glands, there was an apparent increase in the number of ERα$^+$ cells (Figure 5.8B). Quantification of ERα$^+$ luminal cells showed that 49.0 $\pm$ 8.8% of luminal cells were ERα$^+$ in the *Bcl11a*-deficient virgin glands (n=2) compared to 25.0 $\pm$ 7.1% in control glands (n=2). Since ERα was not increased in RT-PCR (See below, Figure 5.11), this result indicated a selective loss of the ERα$^-$ cells in the *Bcl11a*-deficient virgin glands. Consistent with this result, only the Sca1$^-$ (ERα$^-$) population showed decreased mammary colony-forming cell (Ma-CFC) capabilities upon *Bcl11a* deletion (Appendix A.8). The Sca1$^+$ (ERα$^+$) luminal progenitors, on the other

hand did not show any significant reduction in Ma-CFC capabilities (Appendix A.8). Taken together, these results suggest that deletion of *Bcl11a* results in the loss of $Sca1^-$ ($ER\alpha^-$) luminal cells, hence leading to a relative increase in the percentage of $ER\alpha^+$ luminal cells and dysregulating the balance between the $ER\alpha^+$ and $ER\alpha^-$ luminal cells.

In the *Gata-3* conditional knockout mice, deletion of *Gata-3* in the mammary glands resulted in a loss of $ER\alpha^+$ luminal cells (Asselin-Labat et al., 2007; Kouros-Mehr et al., 2006). This suggests that there may be an $ER\alpha^+$ luminal population which is not affected by loss of *Bcl11a* and *Gata-3*. Alternatively, this suggests that Gata3 might not the primary effector of Bcl11a in the virgin gland or that these *Bcl11a*-deficient $ER\alpha^+$ luminal cells no longer depend on *Gata-3*.

Over-expression of Notch intracellular domains impairs mammary ductal growth and causes dilated ducts in virgin glands (Hu et al., 2006; Jhappan et al., 1992). Our lab had previously showed that the T-cell leukaemia phenotypes observed in the *Bcl11a* mutant lymphocytes might be caused by abnormal Notch signalling (Liu et al., 2003b). I thus examined whether there was altered expression of components of the Notch pathway in the *Bcl11a*-deficient virgin glands. Immunohistochemistry for Notch1 and its ligand, Jagged1 showed a clear increase of Notch1 and a modest increase of Jagged1 expression in the sections of the *Bcl11a*-deficient virgin glands (Figure 5.9A and 5.9B). Therefore deletion of *Bcl11a* in the virgin gland appeared to lead to aberrant activation of the Notch pathway.

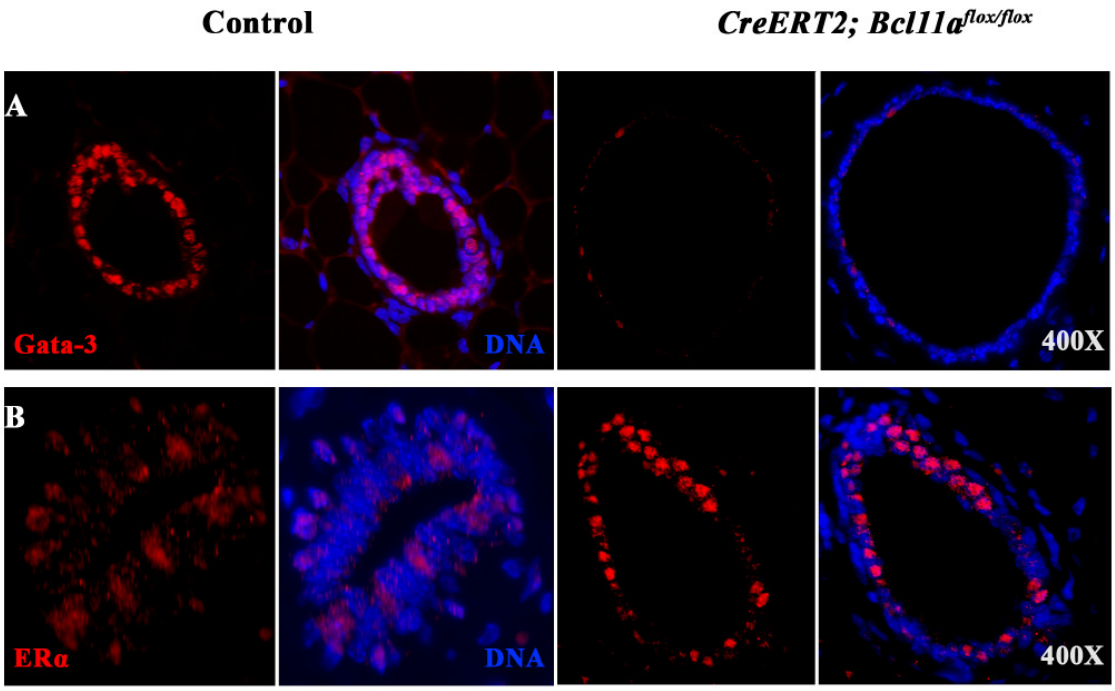

Figure 5.8. Immunohistochemical analysis of tamoxifen treated control and *Cre-ERT2; Bcl11a*$^{flox/flox}$ mammary glands. Immunostaining of sections using antibodies against **(A)** Gata-3 and **(B)** ERα. Control: Wild-type/*CreERT2*; *Bcl11a*$^{flox/+}$.

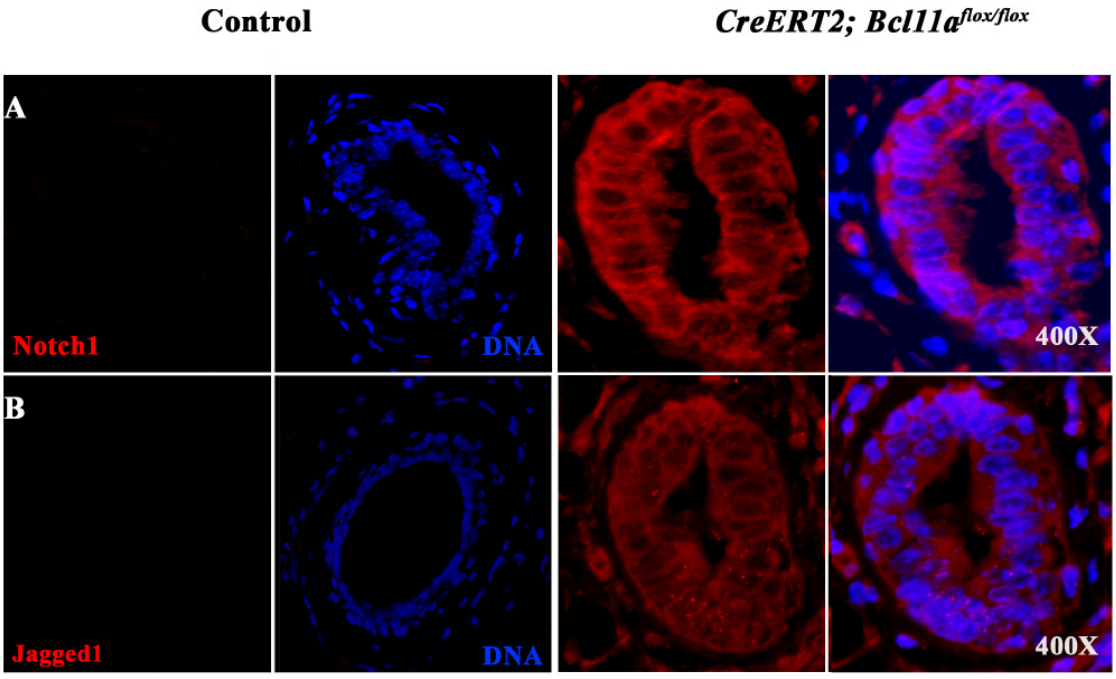

Figure 5.9. Immunohistochemical analysis of tamoxifen treated control and *Cre-ERT2; Bcl11a*$^{flox/flox}$ mammary glands sections using additional markers. Immunostaining of sections using antibodies against **(A)** Notch1 and **(B)** Jagged1. Control: Wild-type/*CreERT2*; *Bcl11a*$^{flox/+}$.

5.2.5 *Bcl11a*-deficient virgin glands exhibit a shift towards luminal profile

Notch signalling has been suggested to influence lineage specification of the mammary epithelium (Buono et al., 2006; Smith et al., 1995). Given that the deletion of *Bcl11a* disrupted ductal architecture and resulted in ectopic activation of Notch signalling, I stained the mammary epithelial cells with antibodies to cell surface markers CD24 and CD49f and analyzed them by flow cytometry. The total percentage of epithelial cells ($CD24^+$) in *Bcl11a*-deficient mammary glands was slightly decreased (12.99 $\pm$ 0.45% compared to 15.65 $\pm$ 0.35% in the control glands; n=3). In the control glands (n=3), luminal ($CD24^{hi}CD49f^+$) and basal cells ($CD24^+CD49f^{hi}$) accounted for about 5.0 $\pm$ 1.6% and 5.7 $\pm$ 1.8% of total Lin^- cells respectively. Loss of *Bcl11a* resulted in an increase in the percentage of $CD24^{hi}CD49f^+$ luminal cells (8.80 $\pm$ 1.0%), and a decrease in percentage of $CD24^+CD49f^{hi}$ basal cells (2.56 $\pm$ 0.2%) (n=3) (Figure 5.10). Since most of the Gata-3-expressing cells were lost in the *Bcl11a*-deficient gland, the higher percentage of $CD24^{hi}CD49f^+$ luminal cells most likely reflected the relative increase of more differentiated $ER\alpha^+$ luminal cells rather than a general increase of total luminal cells.

To further interrogate the molecular changes, I analyzed gene expression changes in the *Bcl11a*-deficient virgin glands using RT-PCR. As shown in Figure 5.11, there was reduction in expression of luminal (*NKCC1*, *Muc1*) and basal (*CK14*) markers in the *Bcl11a*-deficient mammary glands, indicating the important roles of Bcl11a in both luminal and basal lineages. Additionally, consistent with the immunohistochemistry results, *Gata-3* expression was significantly reduced and *Bcl11b* and *Notch1* expression were clearly increased in the *Bcl11a*-deficient mammary glands. *ERα* expression however, was not significantly reduced compared to *Muc1* and *NKCC1*, further highlighting the selective depletion of the $ER\alpha^-$ cells. Elf5 is a key player in alveolar cell fate specification and is expressed at low levels in the virgin gland. *Bcl11a* deletion caused a near complete loss of *Elf5* expression. This result, and the selective depletion of $ER\alpha^-$ cells, suggested a likely loss of alveolar progenitors when *Bcl11a* was deleted.

These phenotypes in the virgin glands have clearly established that *Bcl11a* is a critical regulator in normal mammary development.

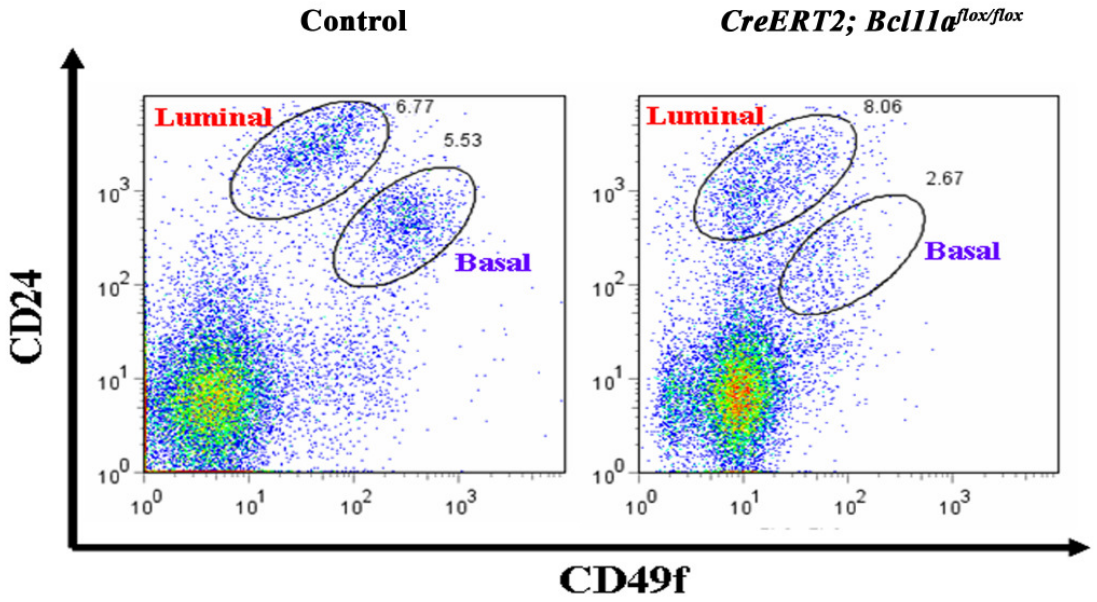

Figure 5.10. Mammary FACS profile of tamoxifen treated control and *Cre-ERT2; Bcl11a*$^{flox/flox}$ mammary glands. Flow cytometric analysis of isolated epithelial cells using CD24 and CD49f markers. There is an increase in the percentage of luminal cells (CD24^{hi}CD49f^{+}) in the *Bcl11a*-deficent glands compared to the control glands (n=3). Control: Wild-type/*CreERT2*; *Bcl11a*$^{flox/+}$.

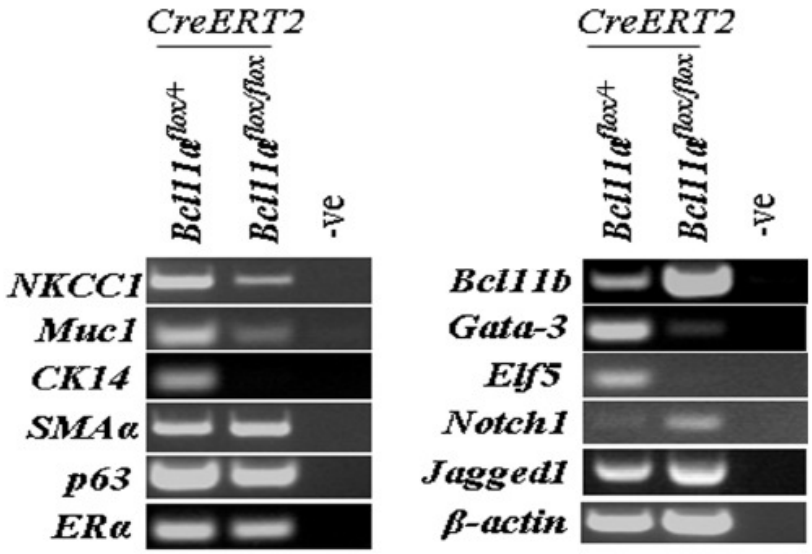

Figure 5.11. Analysis of tamoxifen treated control and *Cre-ERT2; Bcl11a*$^{flox/flox}$ whole mammary glands using semi-quantitative RT-PCR. RT-PCR shows a decrease in levels of both luminal and basal markers and up-regulation of Notch receptors in the *Bcl11a*-deficient glands. β-actin is used as a control. Control: Wild-type/*CreERT2*; *Bcl11a*$^{flox/+}$. –ve indicates no template control.

5.2.6 Loss of *Bcl11b* in virgin glands results in precocious alveolar development

To investigate the function of *Bcl11b* in the virgin mammary gland, I administered TAM to 4-8-week-old *CreERT2; Bcl11b*$^{flox/flox}$ and control (*Bcl11b*$^{flox/+}$ heterozygous and wild-type) females to induce *Bcl11b* deletion. The injected mice were analyzed three weeks post injection. Genomic DNA was extracted from TAM-injected mammary glands and Cre-mediated excision was detected using PCR primers as shown in Figure 5.12A. Cre-mediated excision of *Bcl11b* was confirmed by the presence of deletion bands in the mammary glands (Figure 5.12B) and quantitative real time PCR (qRT-PCR) amplification of genomic DNA derived from these mammary glands showed that the deletion efficiency was ~60%. In addition, mammary epithelial cells were sorted into luminal ($CD24^{hi}CD49f^{+}$) and basal ($CD24^{+}CD49f^{hi}$) fractions using FACS and genomic DNA was extracted and Cre-mediated excision of *Bcl11b* was again confirmed by the presence of deletion bands (Figure 5.12C).

Strikingly, deletion of *Bcl11b* resulted in pregnancy-like alveologenesis in the virgin glands (Figure 5.13A). Numerous alveolar structures developed along the primary ducts of the *Bcl11b*-deficient virgin glands and histological examination revealed that these alveoli resembled that of a wild-type day 10 gestation mammary gland (Figure 5.13B-C). To confirm that the alveoli in the *Bcl11b*-deficient virgin glands had indeed undergone secretory differentiation, I stained sections of the glands with an antibody to β-casein. As shown in Figure 5.14A, β-casein producing cells were present in the *Bcl11b*-deficient virgin glands but not in the control glands, indicating that loss of *Bcl11b* resulted in proliferation and differentiation of luminal (ductal and alveoli) mammary epithelial cells normally only found in the pregnant gland. Immunostaining with anti-Aquaporin 5 antibody showed that Aquaporin 5 was not detected in *Bcl11b*-deficient virgin glands even in ducts (Figure 5.14B), a phenomenon similar to the wild-type mid-gestation mammary glands (Shillingford et al., 2003). To further investigate the mammary defects, I examined additional markers of luminal (CK18) and basal (p63 and SMA) cells using immunohistochemistry. The alveolar-like structures in the *Bcl11b*-deficient glands expressed basal markers p63 and SMA in the outer layer, as well as CK18 in the luminal cells (Figure 5.14B-E), suggesting that the mammary architecture of

Bcl11b-deficient glands were similar to that wild-type mid-gestation glands. Interestingly, some of the p63 positive cells appeared to be in the luminal layer (Figure 5.14C).

Activation of Stat5-mediated transcriptional activities by phosphorylation (p-Stat5) is essential for normal lobulo-alveolar cell proliferation and differentiation. Phosphorylation of Stat5 is very low in virgin and during early pregnancy but rises sharply after day 14 of pregnancy (Liu et al., 1997). Immunostaining with antibody to p-Stat5 revealed the absence of p-Stat5 protein in *Bcl11b*-deficient glands (Figure 5.15A), demonstrating that these abnormal glands were earlier than day 14 of pregnancy. In addition, immunostaining with anti-ERα antibodies did not reveal any significant change in the number of $ER\alpha^+$ cells in the mammary ducts (Figure 5.15B). It was noted that there were very few $ER\alpha^+$ cells in the alveolar-like structures in the *Bcl11b*-deficient virgin glands (Figure 5.15B). Next, to determine whether deletion of *Bcl11b* led to abnormal proliferation or cell death, the mammary sections were stained using antibodies to Ki67 and cleaved Caspase 3. No obvious differences between the mutant and the control glands were observed (Figure 5.16A and 5.16B), suggesting that loss of *Bcl11b* did not result in abnormal proliferation or apoptosis of mammary epithelial cells in the virgin glands. However, it was likely that the initial proliferation of epithelial cells to generate the alveolar-like structures had probably occurred before the analysis that was performed 3 weeks after TAM administration.

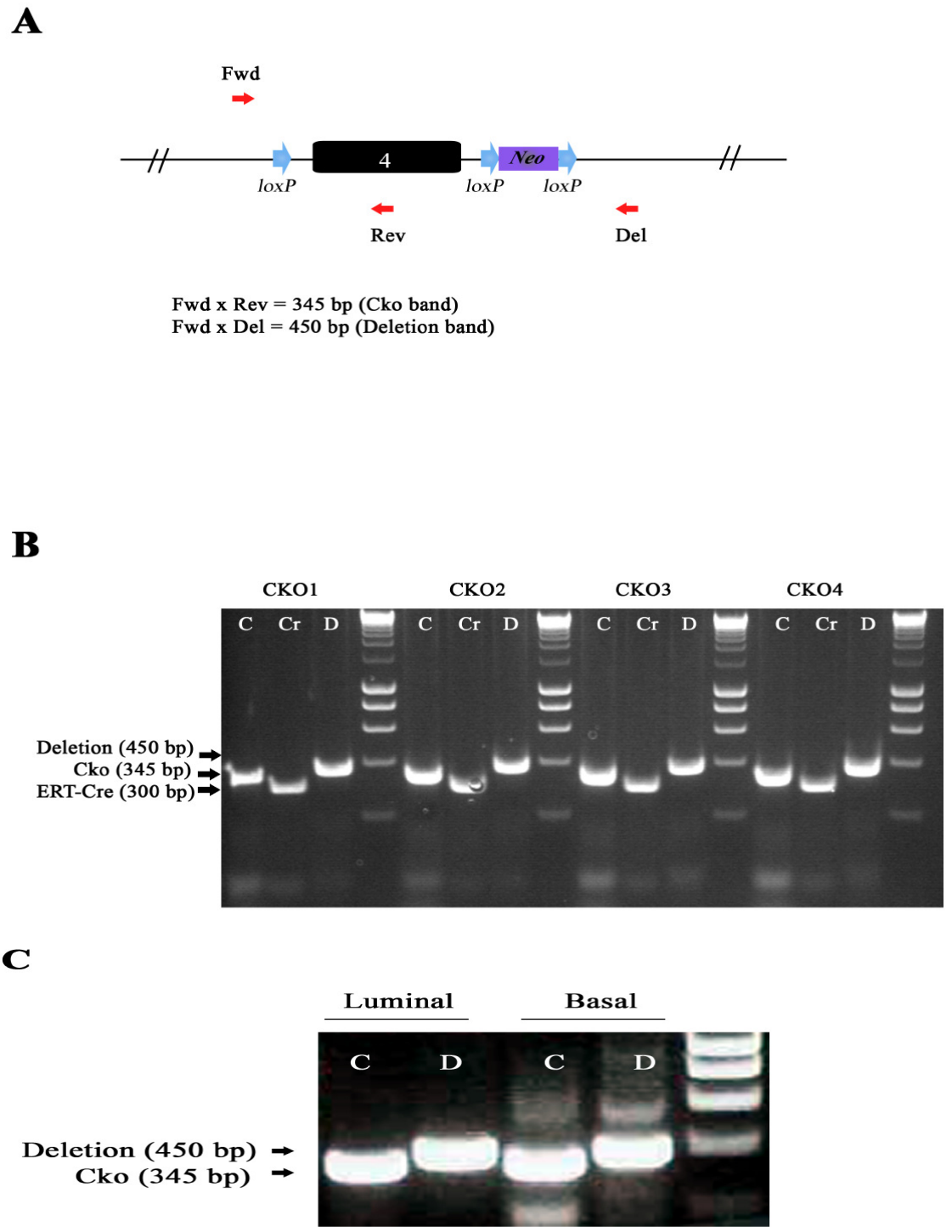

Figure 5.12. Detection of deletion of *Bcl11b* after Cre expression. **(A)** Schematic diagram showing relative position of primers in the *Bcl11b* locus used for detection of deletion band after Cre expression. **(B)** Gel image showing PCR products obtained with primers using genomic DNA extracted from mammary glands of tamoxifen injected *CreERT2*; *Bcl11b*$^{flox/flox}$ mice. **(C)** Gel image showing PCR products obtained from genomic DNA extracted from sorted luminal (CD24^{hi}/CD49f^{+}) and basal (CD24^{+}/CD49f^{hi}) epithelial cells. CKO1-4 represents mammary glands from four independent mice. C: cko PCR; Cr: Cre PCR; D: Deletion PCR.

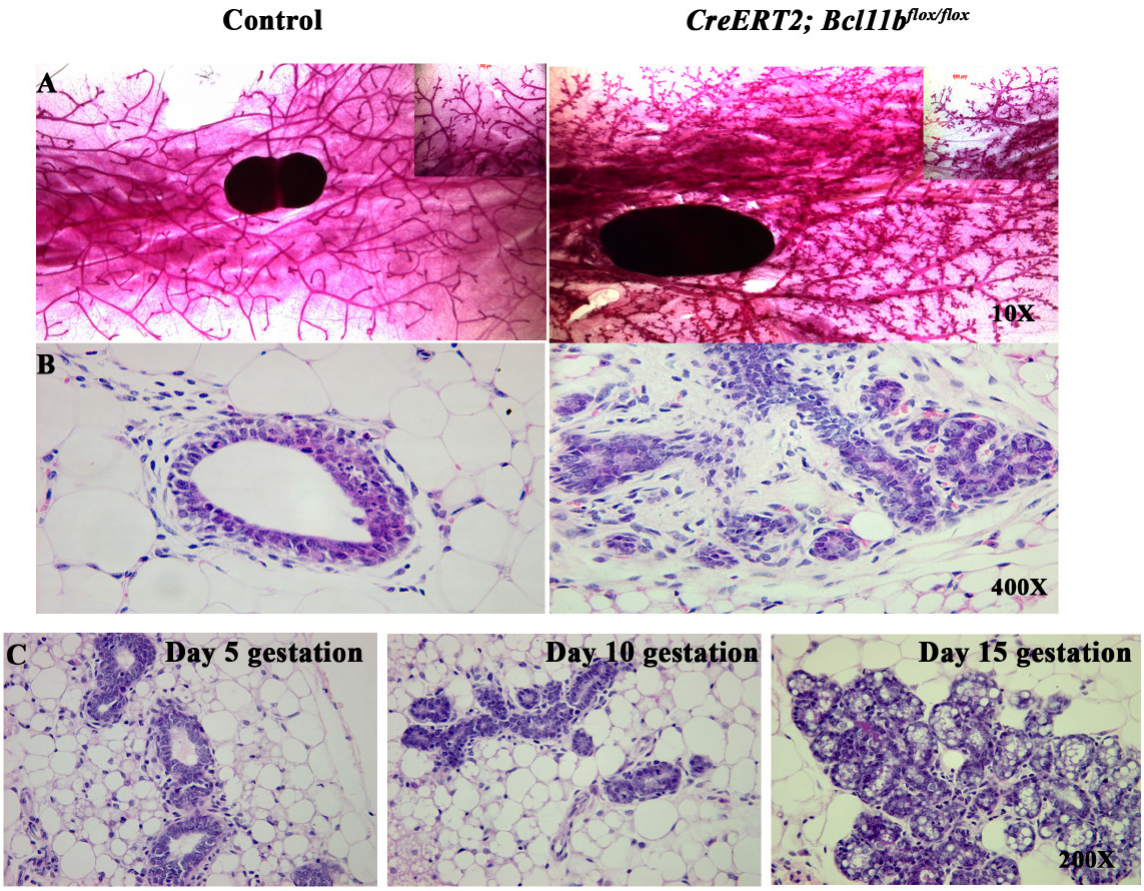

Figure 5.13. Morphological analysis of tamoxifen treated control and *Cre-ERT2; Bcl11b*$^{flox/flox}$ mammary glands. (A) Whole mount carmine alum-stained and **(B)** H&E stained sections of TAM injected control (Wild-type/*CreERT2*; *Bcl11b*$^{flox/+}$) and *CreERT2*; *Bcl11b*$^{flox/flox}$ mammary glands. **(C)** H&E stained sections of day 5/10/15 gestation wild-type mammary glands. The *Bcl11b*-deficient virgin glands resemble that of a day 10 gestation gland.

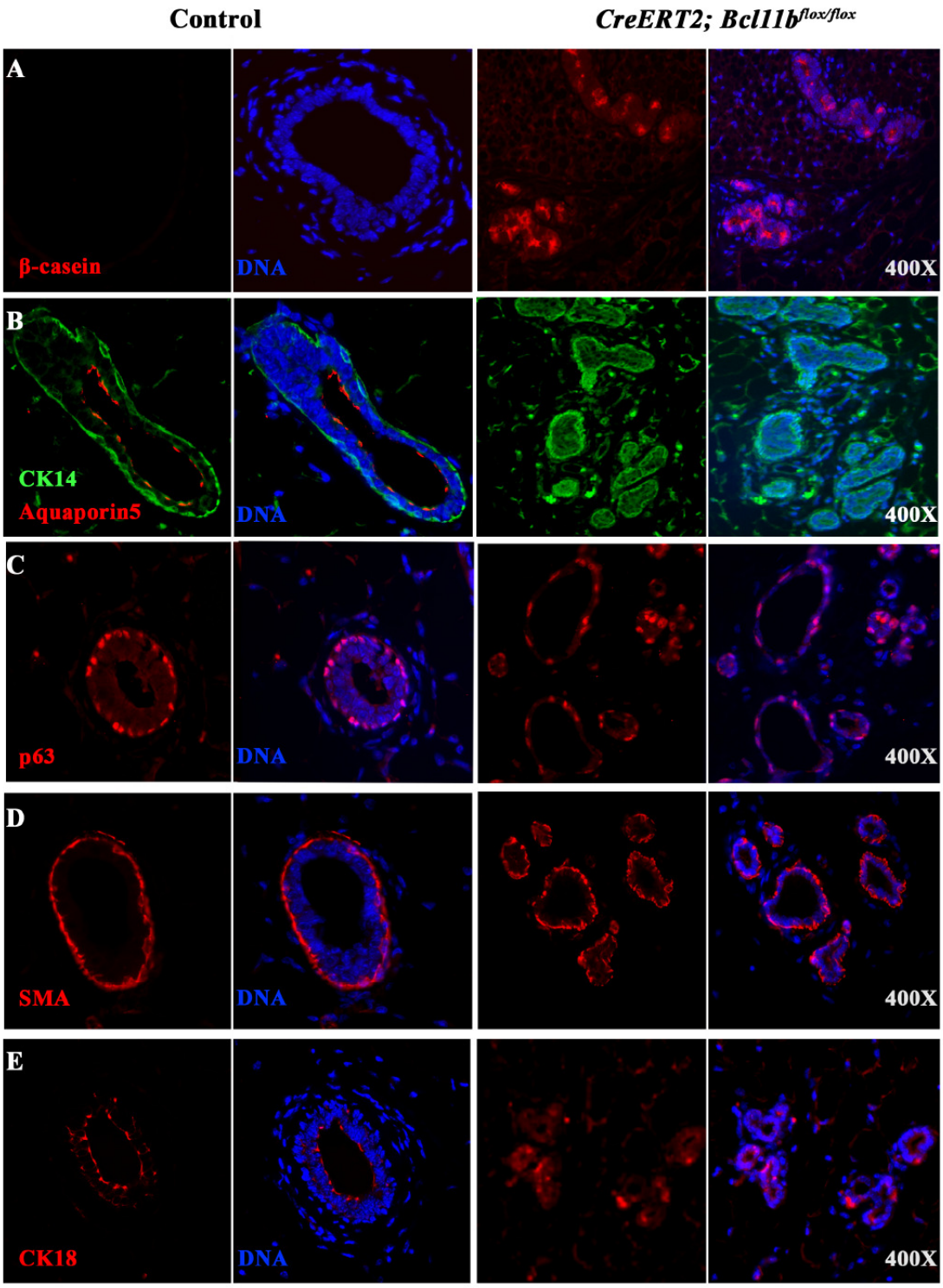

Figure 5.14. Immunohistochemical analysis of tamoxifen treated control and *Cre-ERT2; Bcl11b*$^{flox/flox}$ mammary glands sections using luminal/basal markers. Immunostaining of sections using antibodies against **(A)** β-casein, **(B)** Aquaporin 5, CK14, **(C)** p63, **(D)** SMA and **(E)** CK18. Control: Wild-type/*CreERT2*; *Bcl11b*$^{flox/+}$. Note: Images from control panels were the same as that used for Figure 5.6.

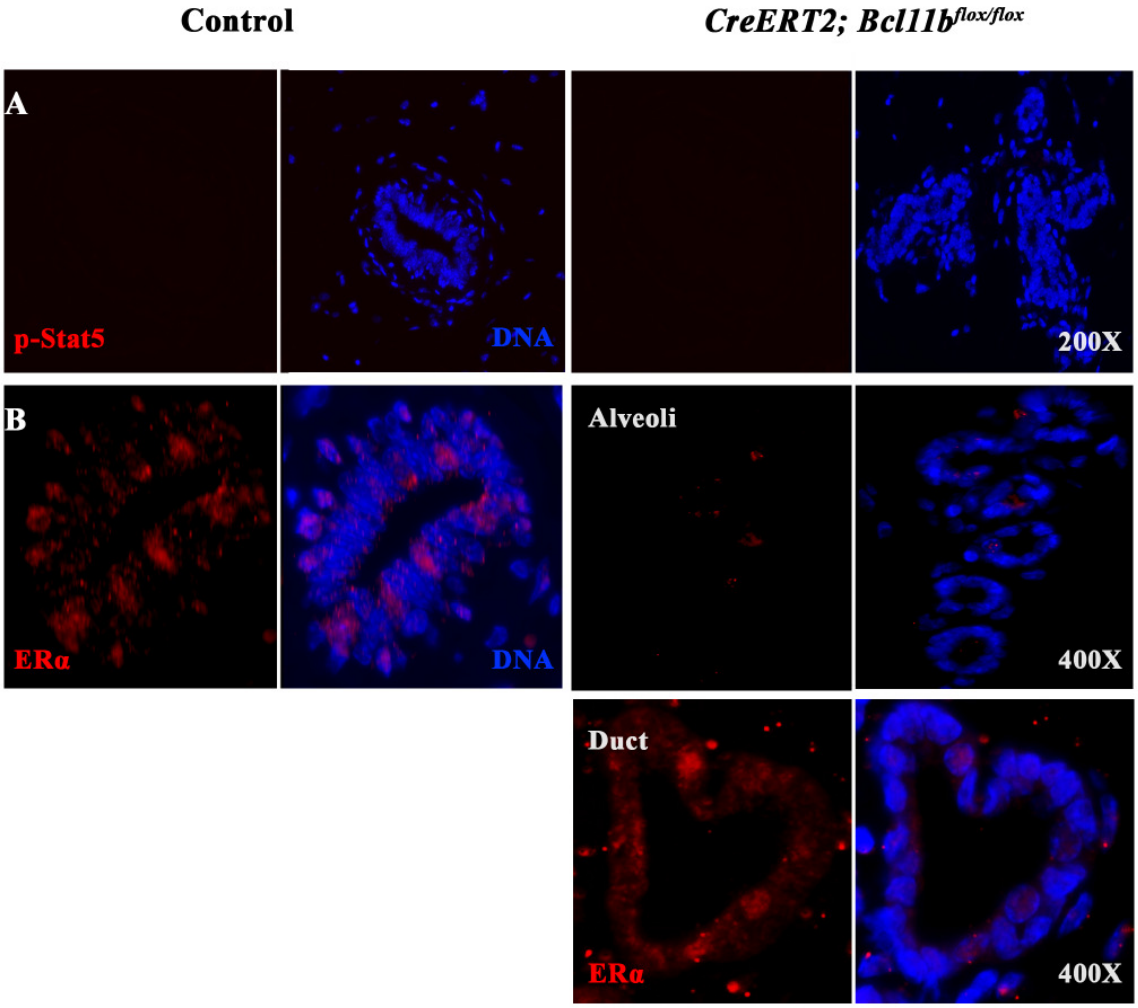

Figure 5.15. Immunohistochemical analysis of tamoxifen treated control and *Cre-ERT2; Bcl11b*$^{flox/flox}$ mammary glands. Immunostaining of sections using antibodies against **(A)** p-Stat5 and **(B)** ERα. Control: Wild-type/*CreERT2*; *Bcl11b*$^{flox/+}$. Note: Images from control panels were the same as that used for Figure 5.8B.

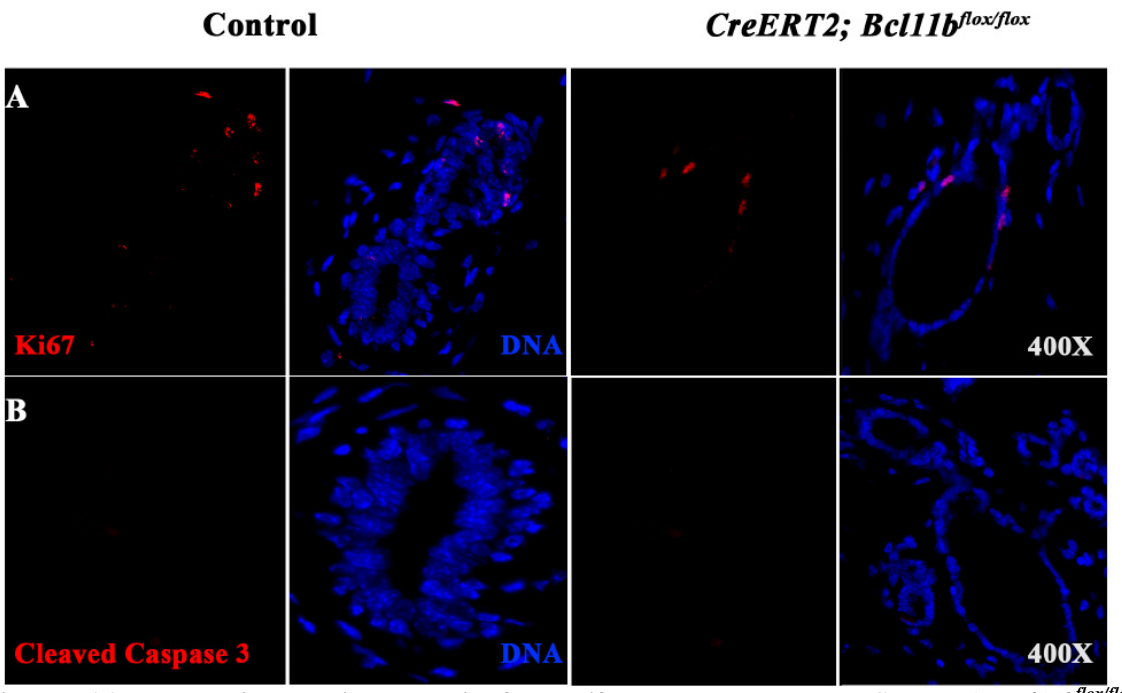

Figure 5.16. Immunohistochemical analysis of tamoxifen treated control and *Cre-ERT2; Bcl11b*$^{flox/flox}$ mammary glands sections using additional markers. Immunostaining of sections using antibodies against **(A)** Ki67 and **(B)** Cleaved Caspase 3. Control: Wild-type/*CreERT2*; *Bcl11b*$^{flox/+}$. Note: Images from control panels were the same as that used for Figure 5.7.

5.2.7 Basal fractions of *Bcl11b*-deficient virgin glands express luminal markers

To determine if loss of *Bcl11b* altered the proportion of luminal and basal cells within the mammary epithelium, mammary epithelial cells were stained using the antibodies to CD24 and CD49f and analyzed by flow cytometry. There was an increase in the total percentage of epithelial cells ($CD24^+$) in the *Bcl11b*-deficient mammary glands (22.5 $\pm$ 5.48% compared to 15.65 $\pm$ 0.35% in the control glands; n=3). Interestingly, the *Bcl11b*-deficient glands (n=3) showed an increase in the percentage of $CD24^+CD49f^{hi}$ (basal) cells (15.3 $\pm$ 5.4% compared to 5.7 $\pm$ 1.8% in the control glands), accompanied with a drastic reduction in the percentage of $CD24^{hi}CD49f^+$ (luminal) cells (1.8 $\pm$ 0.5% compared to 5.0 $\pm$ 1.6% in the control glands) (Figure 5.17). The expansion of basal fraction was unexpected as phenotypic analyses showed that loss of *Bcl11b* resulted in luminal differentiation and development of a pregnancy-like mammary gland (Figure 5.13); hence an increase in the luminal fraction was expected. In order to examine the identity of the basal population of *Bcl11b*-deficient glands, I sorted this basal fraction ($CD24^+CD49f^{hi}$) and performed RT-PCR to determine expression of various lineage markers. Strikingly, I found that these basal cells expressed typical luminal markers such as *NKCC1* along with milk protein genes *α-casein* and *β-casein*, in addition to the basal genes *CK14*, *SMA* and *p63* (Figure 5.18). Moreover, *Gata-3*, *Notch1* and *Notch3* which were normally only expressed in luminal cells, were now detected in the basal fractions of *Bcl11b*–deficient mammary glands (Figure 5.18). Since *Bcl11b* was predominantly expressed in basal cells, these results demonstrated that these *Bcl11b*–deficient basal cells had acquired luminal properties and that the CD24 and CD49f flow cytometric profile no longer faithfully represented basal or luminal cells under this particular condition. The switch from basal cells to luminal alveolar cells was not complete since these cells did not express *Elf5*, a key gene in specifying alveolar cell fate, nor did they have increased *Bcl11a* expression (Figure 5.18). Taken together, these results suggest that *Bcl11b* maintains basal identity and suppresses luminal cell fate.

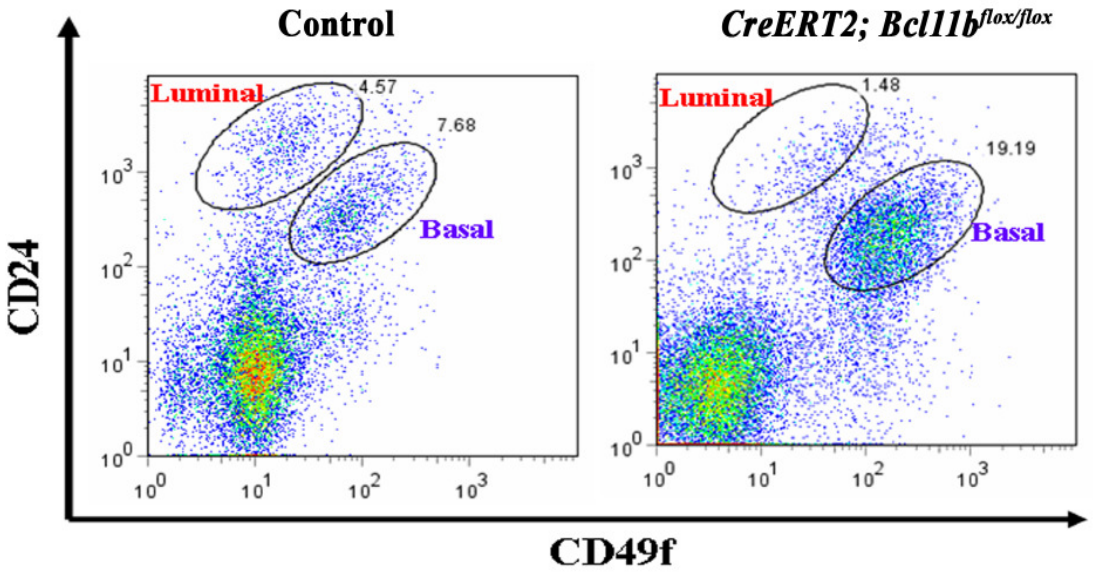

Figure 5.17. Mammary FACS profile of tamoxifen treated control and *Cre-ERT2; Bcl11b*$^{flox/flox}$ mammary glands. Flow cytometric analysis of isolated epithelial cells using CD24 and CD49f markers. There is an increase in the percentage of basal cells ($CD24^{+}CD49f^{hi}$) in the *Bcl11b*-deficent glands compared to the control glands (n=3). Control: Wild-type/*CreERT2*; *Bcl11b*$^{flox/+}$.

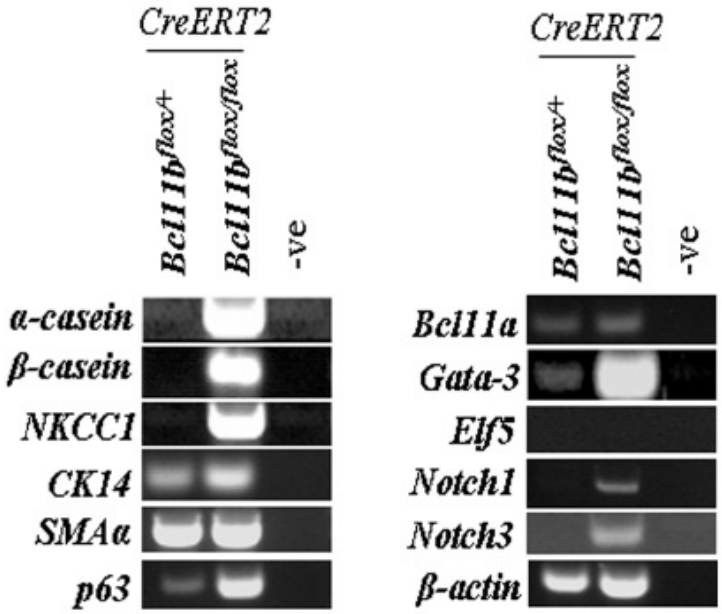

Figure 5.18. Analysis of sorted basal cells from tamoxifen treated control and *Cre-ERT2; Bcl11b*$^{flox/flox}$ mammary glands using semi-quantitative RT-PCR. The $CD24^{+}CD49f^{hi}$ basal cells are sorted out and RT-PCR shows the expression of luminal markers within this fraction of the *Bcl11b*-deficient glands. In addition, Notch receptors which are normally expressed in luminal cells are also detected in the basal fraction. β-actin is used as a control. Control: Wild-type/*CreERT2*; *Bcl11b*$^{flox/+}$. –ve indicates no template control.

5.2.8 *Bcl11b* promotes basal identity in mammary epithelial cells

Expression of *Bcl11b* was detected predominantly in basal cells and in a small number of $Sca1^-$ luminal progenitors in the virgin glands. The results from the loss-of-function studies demonstrated that *Bcl11b* maintains basal identity and suppresses luminal identity and differentiation. Deletion of *Bcl11b* led to the abnormal proliferation and/or differentiation, resulting in a "pregnancy-like" phenotype. To determine whether *Bcl11b* promotes the basal lineage, I over-expressed *Bcl11b* using the over-expression vectors (as described in Appendix A.7) in the murine mammary epithelial cell line, KIM2 (maintained by Dr Walid Khaled) (Gordon et al., 2000). As shown in Figure 5.19, transient over-expression of *Bcl11b* in KIM2 resulted in up-regulation of basal markers such as *CK14*, *p63* and *SMA* but not luminal markers *Gata-3* and *Elf5*, indicating that expression of *Bcl11b* alone induced expression of basal markers in epithelial cells.

In collaboration with Dr Walid Khaled (who performed the experiments), we analyzed the *Stat6*$^{-/-}$ knockout mice that have a delay in alveologenesis during early gestation (Khaled et al., 2007). An increase in the levels of *Bcl11b* in the luminal ($CD24^{hi}CD49f^+$) cells of the virgin and day 5 gestation glands from *Stat6*$^{-/-}$ knockout mice compared to wild-type controls was observed (Figure 5.20A). We quantified the levels of *Bcl11* genes in the luminal ($CD24^{hi}CD49f^+$) and basal ($CD24^+CD49f^{hi}$) fractions using qRT-PCR and found that there was a 74-fold increase in *Bcl11b* expression in the luminal cells of the $Stat6^{-/-}$ virgin mice compared to wild-type controls (Figure 5.20B). When the mammary colony-forming cell (Ma-CFC) capabilities of the luminal progenitors were assessed and compared to the wild-type controls, a significant reduction in Ma-CFC capabilities of *Stat6*$^{-/-}$ luminal progenitors was observed (Figure 5.20C). These data indicated that the increased expression of *Bcl11b* was associated with the decrease in Ma-CFC capabilities of luminal progenitors and the alveologenesis defects in *Stat6*$^{-/-}$ mammary glands. Taken together, these data demonstrate that *Bcl11b* maintains basal cell fate and acts as a suppressor to luminal differentiation and/or luminal cell fate.

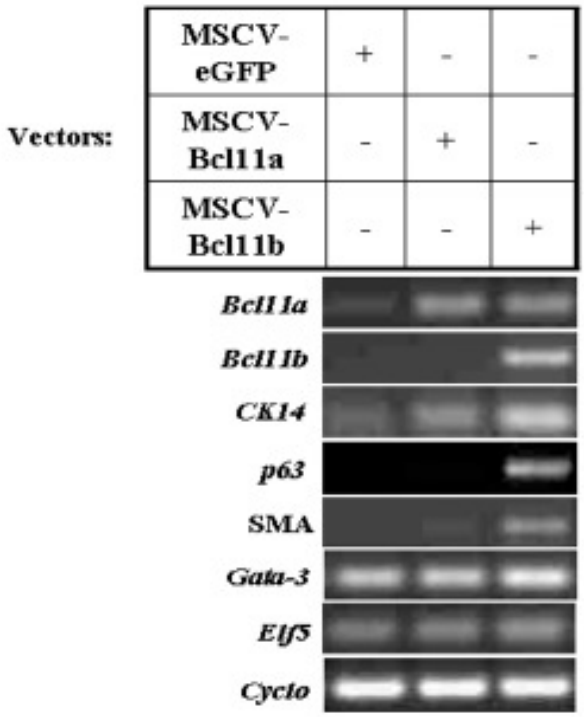

Figure 5.19. Over-expression of *Bcl11* genes in mammary epithelial cell line, KIM2. Over-expression of *Bcl11b* in KIM2 cells results in up-regulation of basal markers (*p63*, *CK14* and *SMA*) as determined by RT-PCR. In contrast, expression of *Gata-3* and *Elf5* remains unchanged. No changes in the expression of the examined markers are observed in KIM2 cells transfected with MSCV-Bcl11a. MSCV-eGFP vector is used as the transfection control. + indicates vector used for each transfection; - indicates vector not used for transfection. Cyclophilin A is used as a control for RT-PCR.

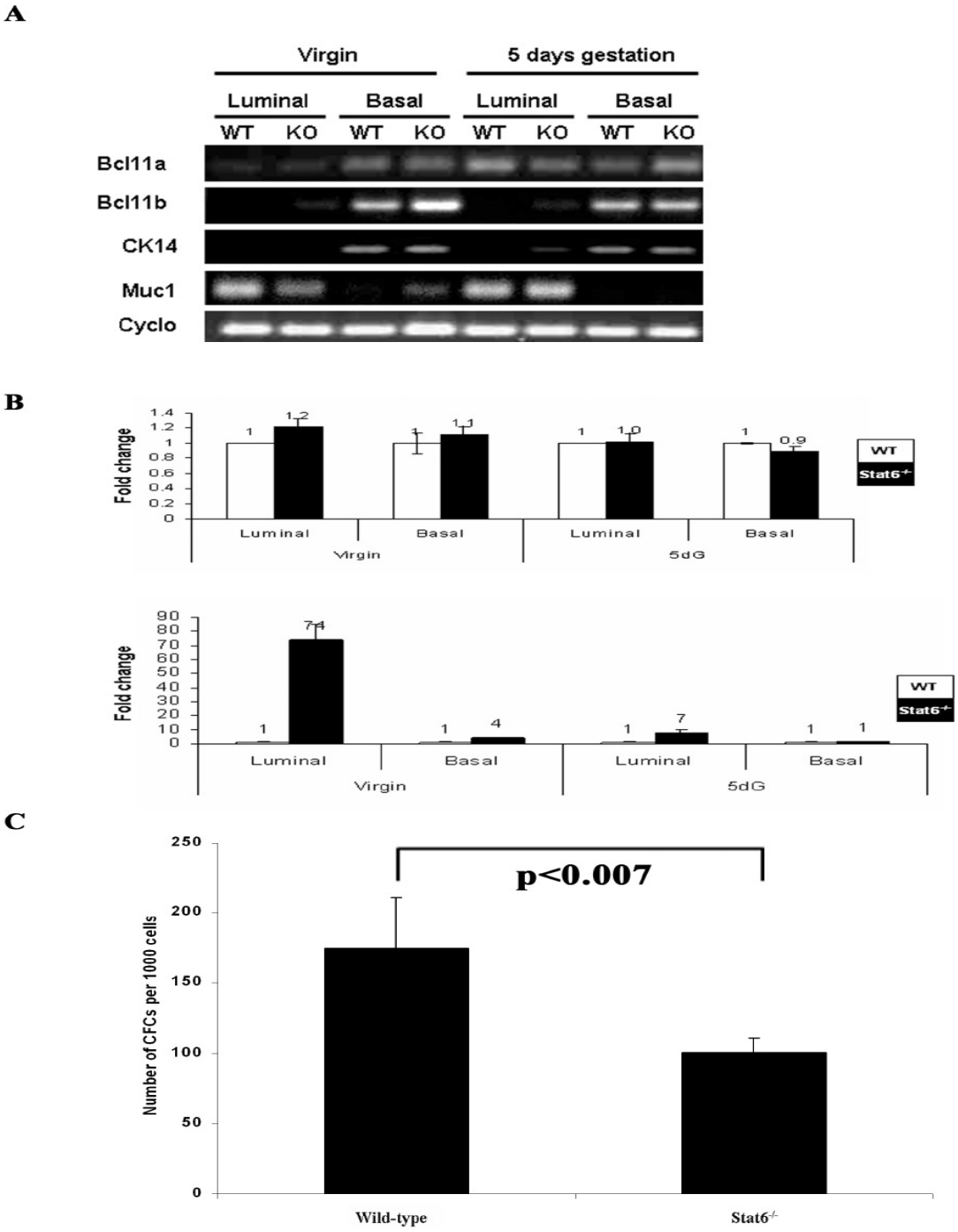

Figure 5.20. Analysis of mammary glands from *Stat6*$^{-/-}$ virgin and day 5 gestation female mice. (A) Semi-quantitative RT-PCR analysis of the luminal ($CD24^{hi}CD49f^{+}$) and basal ($CD24^{+}CD49f^{hi}$) fractions of wild-type and *Stat6*$^{-/-}$ mammary glands. Up-regulation of *Bcl11b* expression is observed in the luminal fractions of *Stat6*$^{-/-}$ mammary glands. **(B)** Quantitative real time PCR analysis of *Bcl11a* and *Bcl11b* expression in sorted luminal ($CD24^{hi}CD49f^{+}$) and basal ($CD24^{+}CD49f^{hi}$) cells of *Stat6*$^{-/-}$ and wild-type mammary glands. A 74-fold increase in *Bcl11b* expression is observed in luminal cells of the *Stat6*$^{-/-}$ virgin gland. **(C)** Mammary colony-forming cell (Ma-CFC) assay of sorted $CD24^{hi}CD49b^{+}$ cells (luminal progenitors) from either wild-type or *Stat6*$^{-/-}$ virgin glands. A 40% reduction in Ma-CFCs (per 1000 cells) is observed in the *Stat6*$^{-/-}$ virgin glands. Error bars denote standard deviation (n=3) and $p<0.007$. WT: Wild-type; KO: *Stat6*$^{-/-}$.

5.3 Discussion

In this Chapter, I demonstrated that *Bcl11a* and *Bcl11b* play important roles in development of the mammary gland. In the embryo, loss of *Bcl11a* resulted in defective mammary buds formation and failure of mammary bud regression in a male embryo. In contrast, loss of *Bcl11b* caused the absence of the third pair of mammary buds and defects in other mammary buds. As *Bcl11* homozygous pups died within 24 hours of birth, conditional knockout alleles of both genes were used to study their roles in postnatal mammary gland development. Condition deletion of *Bcl11a* in the virgin glands disrupted normal mammary bi-layer architecture and resulted in a general loss of mammary epithelial cells. In addition, there was also a loss of $Gata3^+$ cells and a relative increase in the number of $ER\alpha^+$ epithelial cells in the *Bcl11a*-deficient virgin glands. Dysregulation in Notch signalling was also observed in the virgin glands following deletion of *Bcl11a*. Loss of *Bcl11b* on the other hand resulted in precocious alveologenesis and lineage alteration in the virgin glands. Gain-of-function studies also indicated the essential role of *Bcl11b* in promoting basal lineage. Increased levels of *Bcl11b* in luminal progenitors were associated with a dramatic decrease in Ma-CFCs capabilities. Over-expression of *Bcl11b* in mammary epithelial cells resulted in up-regulation of basal markers. Taken together, these results demonstrate the essential roles of *Bcl11* genes in normal mammopoiesis and lineage commitment, suggesting that the interplay between the two genes is critical for the regulation of mammary epithelial cell fate.

5.3.1 *Bcl11* genes are important for embryonic mammary development

The embryonic mammary gland develops via extensive epithelial-mesenchymal interactions, similar to other skin appendages such as the hair follicles and teeth (Mikkola and Millar, 2006). Mammary bud formation was detected in the $Bcl11a^{lacZ/lacZ}$ homozygous mutant embryos using the antisense *Fgfr2TK* probe. No missing buds were observed in all the mutants analysed. This was consistent with the expression of *Bcl11a* that was only detected in the mammary anlage from 13.5 dpc onwards. This indicated that loss of *Bcl11a* did not affect the inductive signals required for the initial formation of

the mammary placodes. Further analyses using other *in situ* markers showed that the mammary buds formed in the *Bcl11a*$^{lacZ/lacZ}$ homozygous mutant 13.5-14 dpc embryos had a flattened morphology whereas those in the wild-type embryos were visible as elevated knob-liked structures. Expression of *Bcl11a* was detected in both the mammary epithelium and the surrounding mesenchyme. Epithelial-mesenchymal interactions are important for the proper formation of the mammary anlage. The mesenchyme may at least have a permissive function for the induction of mammogenesis (Veltmaat et al., 2003). Mesenchyme from the mammary region of a 13 dpc mouse embryo induces functional mammary epithelium in rat midventral or dorsal epidermis (Cunha and Hom, 1996). Furthermore, the mesenchyme still retains its inductive capacity for placode formation even after the stage of placode induction. Thus the mammary mesenchyme also provides an instructive signal for mammary placode formation and suggests that placode formation is not an intrinsic property of the epithelium of the mammary region. Therefore, the phenotype observed in *Bcl11a*$^{lacZ/lacZ}$ homozygous mutant 13.5-14 dpc embryos might be a result of defective epithelial-mesenchymal interactions and/or signalling, though further studies are needed to ascertain this.

Consistent with a previous study which showed that by 14.5-15.5 dpc, *Lef1* expression becomes undetectable in the epidermis destined to become nipple sheath (Foley et al., 2001), expression of *Lef1* was not detected in all the buds with the exception of the fifth pair of the wild-type 14.5 dpc embryos. In contrast, expression of *Lef1* was observed in all the mammary epidermis of *Bcl11a*$^{lacZ/lacZ}$ homozygous mutant embryos at 14.5 dpc. Furthermore, presence of rudimentary mammary buds in a *Bcl11a*$^{lacZ/lacZ}$ homozygous mutant male embryo at 16.5 dpc was detected using *in situ* hybridization with antisense *Fgfr2TK* probe, suggesting that loss of *Bcl11a* resulted in failure of regression of mammary buds. Whether the continued *Lef1* expression in the mammary epidermis of *Bcl11a*$^{lacZ/lacZ}$ homozygous mutant 14.5 dpc embryos (which might serve as a survival signal), and the failure of regression of mammary buds in the male embryo are causatively linked remains to be determined (Figure 5.21). Determination of the proliferative and apoptotic status of mammary epithelial cells of male embryos between 14.5-16.5 dpc should provide an answer.

Mammary gland development begins at approximately 10.5 dpc with the appearance of milk lines that appear in response to mesenchymal signals (Mailleux et al., 2002; Veltmaat et al., 2004). Interestingly, *Bcl11b* expression was also detected around 10.5 dpc along stripes of ventral lateral surface ectoderm between the fore- and hindlimbs and the expression became localized specifically within the mammary buds from 12.5 dpc. Therefore *Bcl11b* is one of the earliest known mammary lineage markers. Mammary bud formation occurs asynchronously, with the third pair of mammary bud being the first to appear (Mailleux et al., 2002). Studies have also shown that different signals are required for the induction of each pair of placodes (Eblaghie et al., 2004; Mailleux et al., 2002; van Genderen et al., 1994). The importance of *Bcl11b* in embryonic development was underscored by the absence of the third pair of mammary buds in the *Bcl11b* homozygous mutant embryos as indicated by the absence of *Wnt10b* and *Lef1* expression in the presumptive region of the third bud and the reduced *Wnt10b* and *Lef1* expression in other buds at 12.5 dpc. Further examinations of $Bcl11b^{lacZ/lacZ}$ homozygous mutant 14.5 dpc embryos showed that expression of *Fgfr2TK* was reduced in other buds and completely absent in the presumptive third bud region. Hence *Bcl11b* is a specification signal for formation of the third pair of mammary buds. This result also confirms that formation of the third pair of mammary buds is independent of the other buds and requires a different inductive signal.

The genetic hierarchy of *Fgf10* and *Tbx3* remains to be completely elucidated, but the severity of phenotypes in the mutant embryos of either gene where most mammary buds are missing suggests that both of these genes probably lie upstream of *Bcl11b*. Expression of *Fgf10* and *Tbx3*, markers of the mesodermal mammary line, appeared normal in $Bcl11b^{lacZ/lacZ}$ homozygous mutant 10.5 dpc embryos, suggesting that specification of the mammary line itself was not defective. In contrast, expression of *Wnt10b* and *Lef1* was altered in $Bcl11b^{lacZ/lacZ}$ homozygous mutant 12.5 dpc embryos. Hence, it is likely that *Bcl11b* functions upstream of these genes and downstream of *Fgf10* and/or *Tbx3* to relay signals to the precursor mammary epithelial cells (which appear to express *Wnt10b*) (Veltmaat et al., 2004) in order to induce the formation of the third pair of mammary buds (Figure 5.21). Alternatively, *Bcl11b* might also function in a

separate pathway to induce formation of the third pair of mammary buds. Thus, absence of *Bcl11b* resulted in aberrant placode formation off the mammary line.

Loss of the third pair of mammary buds was also observed in the mouse scaramanga (*ska*) mutation (Howard et al., 2005). This mutation has been mapped to the Neuregulin3 (*Nrg3*) gene. In addition, supernumerary glands were formed at high frequency in *ska* mice. *Nrg3* belongs to the neuregulin/heregulin cytokine family and is a direct ligand for the Erbb4 tyrosine kinase receptor. Both *Nrg3* and *Erbb4* are expressed in the presumptive mammary region at 10.75 dpc (Howard et al., 2005). The binding of Nrg3 to Erbb4 results in tyrosine phosphorylation and activation of the receptor leading to activation of downstream signalling cascade. It would be interesting to determine if *Bcl11b* is a target of Nrg3 induced Erbb4 activation in the presumptive third bud region which would explain the observed phenotype. Future experiments can be carried out to determine changes in *Nrg3* expression in $Bcl11b^{lacZ/lacZ}$ homozygous mutant embryos as well as changes in *Bcl11b* expression in *ska* embryos to establish the genetic hierarchy of *Bcl11b* and *Nrg3* in induction of the third pair of mammary buds (Figure 5.21).

In summary, both *Bcl11a* and *Bcl11b* are essential for normal embryonic mammary development.

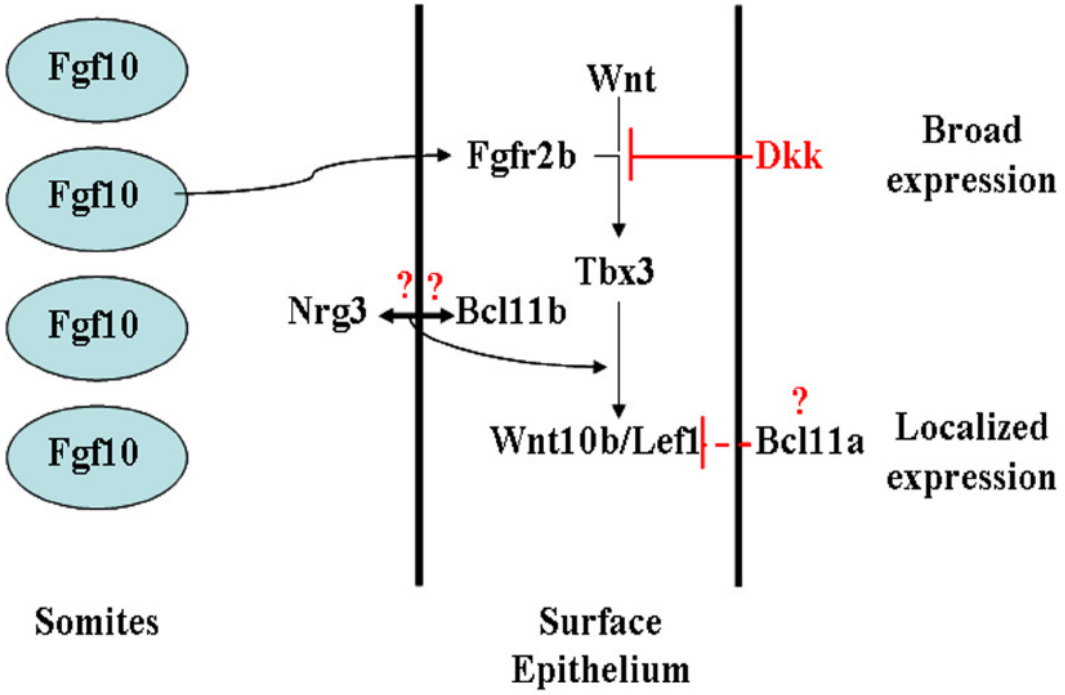

Figure 5.21. Model of possible regulatory factor interactions in the mammary gland. Proposed interactions of *Bcl11* genes within known regulatory networks in embryonic mammary development.

5.3.2 *Bcl11* genes play essential roles in the virgin mammary gland

In the virgin gland, loss of *Bcl11a* caused profound defects in the ductal structure where the mammary architecture was severely disrupted and the luminal and basal cells appeared to form a thin cellular layer in many areas of the ducts. This structural defect was associated with loss of *Gata-3* and *Elf5* expression. Gata-3 and Elf5 are considered to be the key players in luminal specification and alveologenesis. Loss of expression of both genes clearly shows a critical role of Bcl11a in the luminal lineage. Moreover, *Bcl11a* deletion resulted in reduction in expression of several luminal and basal markers, and the *Bcl11a*-deficient epithelium had a lineage shift towards $CD24^{hi}CD49f^{+}$ region in flow cytometric profile, normally considered to be the luminal fraction in the wild-type gland. Relative increase of luminal cells was unexpected since Gata-3 is considered to be the crucial factor in promoting luminal differentiation. It is also surprising that there was a relative increase of the $ER\alpha^{+}$ cells even though Gata-3 expression was lost. Gata-3-expressing cells are mainly $ER\alpha^{+}$ and Gata-3 deletion leads to loss of differentiated cells including the $ER\alpha^{+}$ cells (Asselin-Labat et al., 2007; Kouros-Mehr et al., 2006). This apparent discrepancy is likely to be caused by multiple roles of Bcl11a in several epithelial compartments, which requires further studies. In addition, Bcl11a and Gata-3 are likely to function in distinct epithelial populations or they may act through different pathways. *Bcl11a* is expressed and necessary in the $Sca1^{-}$ luminal progenitors, and is also likely to be expressed in the alveolar progenitors together with *Elf5*. Loss of *Bcl11a* would thus lead to depletion of these progenitors, which are likely to be $ER\alpha^{-}$. Consequently, there would be accumulation of $ER\alpha^{+}$ luminal cell. Alternatively, Bcl11a may play a role in the proposed asymmetric division of $ER\alpha^{-}$ mammary stem cells to produce the $ER\alpha^{+}$ stem/progenitor cells (Asselin-Labat et al., 2006; Booth and Smith, 2006; Dontu et al., 2004; LaMarca and Rosen, 2007; Sleeman et al., 2007). In addition, loss of *Bcl11a* also resulted in decrease in expression of basal markers, suggesting that *Bcl11a* also plays a role in the basal lineage.

Our lab has shown previously that Notch signalling is highly expressed in the *Bcl11a* deficient T-cell leukemia (Liu et al., 2003b). *Bcl11b*, in co-operation with *Notch1* and *Gata3*, is proposed to be the key gene in T cell progenitor commitment to T cell lineage (Rothenberg, 2007a, b), although the definitive evidence is still lacking. In the

virgin mammary glands, loss of *Bcl11a* resulted in increased Notch1 expression. Although *Bcl11a* was expressed primarily in the putative luminal progenitor cells ($CD49b^{+}$), once *Bcl11a* was deleted in the virgin gland, most of the luminal cells appeared to be positive for Notch1, indicating that these luminal cells were likely to be the descendents of the *Bcl11a*-expressing luminal progenitors. Alternatively, non-cell autonomous effects of Notch signalling resulting in the observed phenotypes were also possible. Notch signalling is known to be involved in lineage specification and cell fate determination (Buono et al., 2006; Rothenberg, 2007a). Further studies are needed to investigate the roles of Notch signalling in the mammary gland. Notably, up-regulation of *Bcl11b* was also observed in the *Bcl11a*–deficient mammary glands. The increased level of *Bcl11b* could be partially responsible for the phenotypes in the *Bcl11a* mutant glands. The increased levels of *Bcl11b* could also suggest that there might be a luminal to basal lineage switch as *Bcl11b* was shown to promote basal lineage in this study. Alternatively, the increased levels of *Bcl11b* could be partly responsible for the loss of luminal cells. These possibilities could be investigated using *Bcl11a* and/or *Bcl11b*-over-expressing transgenic mice. Taken together, these results clearly demonstrate that *Bcl11a* is a critical regulator in normal mammary development.

Loss of *Bcl11b* in the virgin gland resulted in precocious alveologenesis and the development of a 'pregnancy-like' state. Histological examination showed the alveolar-like structures developed along primary ducts, and the functional differentiation of luminal cells was confirmed by positive β-casein staining. One remarkable phenotype was that *Bcl11b*-deficient mammary epithelial cells were found within the $CD24^{+}CD49f^{hi}$ (basal) region. It has been observed that differentiated luminal cells from the pregnant glands are fragile and many do not survive the cell dissociation protocol, and are preferentially killed off (Personal communication with John Stingl). This would cause a relative increase in the percentage of $CD24^{+}CD49f^{hi}$ basal cells, resulting in the disparity in the mammary FACS profile observed in the *Bcl11b*-deficient glands. However, expression of luminal (*NKCC1*, *Gata-3*) and milk protein (*α-casein*, *β-casein*) markers was observed in the sorted $CD24^{+}CD49f^{hi}$ (basal) cells of the *Bcl11b*-deficient mammary glands, indicating that these basal cells had acquired luminal properties. Since *Bcl11b* was predominantly expressed in the basal cells, therefore loss of *Bcl11b* in the basal cells

resulted in a lineage switch of some of the basal cells, suggesting that *Bcl11b* normally acts as suppressor to the luminal lineage. These results indicate that *Bcl11b* normally acts as a suppressor to luminal differentiation and blocks precocious alveolar development. Loss of *Bcl11b* would release this brake on luminal differentiation and result in abnormal proliferation and differentiation of luminal cells in the absence of pregnancy hormones. Interestingly, development of these alveolar-like cells was Elf5-independent and did not require increased *Bcl11a* expression, further highlighting the critical role of Bcl11b in maintaining the basal identity. Notably, *Bcl11b* is also expressed in some Sca1$^-$ luminal progenitors. Deletion of *Bcl11b* might also allow the abnormal proliferation and differentiation of these progenitors and eventually contributing to the pregnancy-like phenotype observed. Transplantation of the *Bcl11b*-expressing Sca1$^-$ luminal progenitors into cleared fat-pads and treating the mice with tamoxifen to delete *Bcl11b* will help to clarify this possibility.

Bcl11b not only maintains the basal identity but also promotes the basal lineage. Transient over-expression of *Bcl11b* was sufficient to induce expression of basal cell specific genes such as *CK14*, *p63* and *SMA* in KIM2 mammary epithelial cells (Figure 5.19). In addition, increased levels of *Bcl11b* expression in the luminal progenitors of *Stat6*$^{-/-}$ knockout mice were associated with a dramatic reduction in Ma-CFC capabilities of luminal progenitors (Figure 5.20). In summary, the loss-of-function and gain-of-function analyses clearly demonstrate that *Bcl11b* promotes and maintains the basal lineage and at the same time suppresses luminal cell fate and blocks precocious alveolar development in the virgin mammary gland. Thus the levels of *Bcl11b* are critical to regulate proliferation and differentiation of luminal cells.

The phenotypes following the loss of *Bcl11* genes observed in this study could have arisen due to systemic effects or local stromal effects. This is unlikely as the injected mice were kept within the same cage to minimise the effects of individual female being at a different stage of the estrus cycle. However, to further eliminate any stromal or systemic effects, *Bcl11*-deficient epithelial cells could be transplanted into cleared wild-type mammary fat pads to confirm epithelial contributions to the phenotypes.

5.3.3 Putative roles of *Bcl11* genes in mammary cell fate determination and lineage commitment

Specification, proliferation, differentiation, death and survival of the mammary cells are regulated by networks of information mediated by external signals such as steroids, simple peptide hormones, and by intrinsic cellular factors of various signal pathways(Hennighausen and Robinson, 2005; Watson and Khaled, 2008). Several transcription factors that have been implicated in hematopoietic lineage specification have now been shown to play essential roles in mammary epithelial cell fate decisions (Asselin-Labat et al., 2007; Khaled et al., 2007; Kouros-Mehr et al., 2006). I have now shown that *Bcl11a* and *Bcl11b*, two transcription factors essential in specifying B and T lineages respectively, have critical roles in the mammary epithelium.

The unique expression patterns, phenotypic analysis, and alterations in molecular pathways, have established the roles of both genes at various stages of mammary development (Figure 5.22). *Bcl11a* and *Bcl11b* could be expressed in the multi-potent mammary progenitors since they are among the earliest genes that are specifically expressed in the mammary gland. *Bcl11a* is also expressed in TEBs, in a small number of basal cells of the virgin gland, and deletion of *Bcl11a* results in severe defects in both luminal and basal lineages. From this multi-potent progenitor pool, Bcl11a, working together with Gata-3, promotes the luminal lineage. Although both Bcl11a and Gata-3 are expressed and functional in the luminal progenitors, they have distinct roles. Bcl11a maintains luminal progenitors since *Bcl11a* deletion results in loss of Gata-3 expression and selective depletion of $Sca1^-$ luminal progenitors *in vitro* and $ER\alpha^-$ cells *in vivo*, while Gata-3 primarily promotes progenitor differentiation. *Bcl11a* deletion leads to loss of *Elf5* expression in the virgin gland and reduction of Ma-CFCs. On the other hand, reduction of *Elf5* expression results in accumulation of luminal progenitors, and forced expression of *Elf5* causes reduction of Ma-CFCs. Therefore, it appears that Bcl11a maintains the alveolar progenitors while Elf5 promotes differentiation of this progenitor pool. Similar to *Bcl11a*; *Bcl11b* is also likely to be expressed in the multi-potent progenitors as well. From this progenitor pool, Bcl11b promotes and maintains the basal lineage, and prevents excessive luminal commitment and abnormal differentiation in the absence of pregnancy hormones.

In summary, I have shown that *Bcl11a* and *Bcl11b* are essential for the development, lineage specification and maintenance of the mammary epithelium. In Chapter 6, I will discuss the roles of *Bcl11* genes in maintenance of terminally differentiated luminal secretory cell fate using *Bcl11*$^{flox/flox}$ mice that have been bred to the BLG-Cre mice where Cre recombinase is expressed specifically during lactation (Selbert et al., 1998).

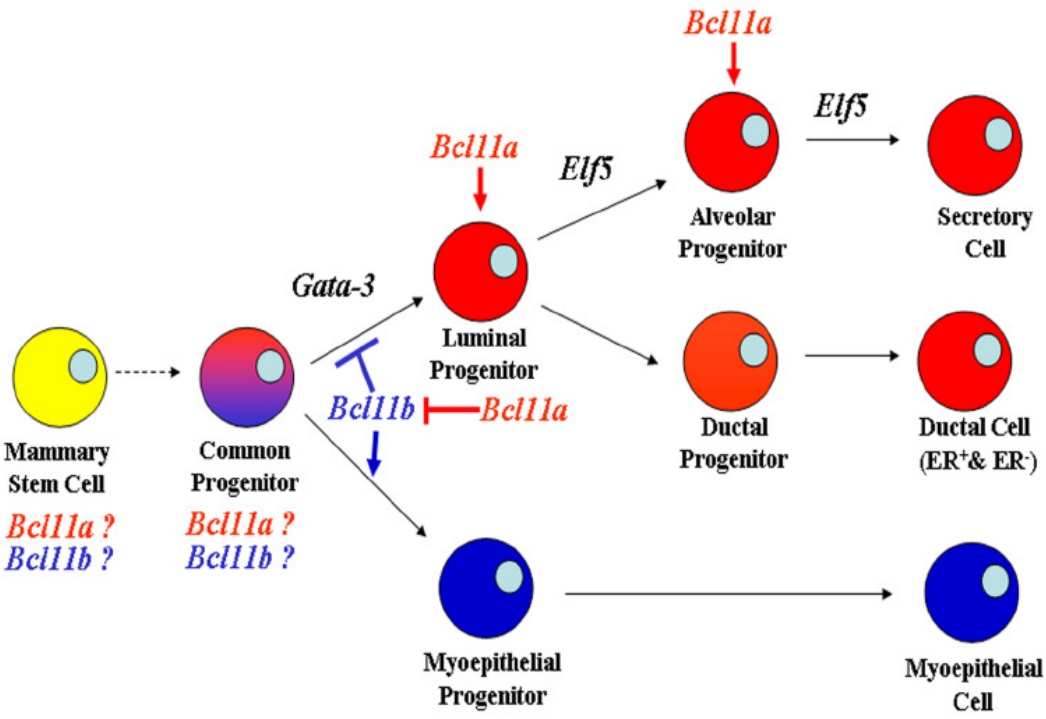

Figure 5.22. Proposed working model of the roles of *Bcl11* genes in mammary lineages. Schematic representation of a model for the roles of *Bcl11* genes in determination of mammary epithelial cell fate determination in relationship to the proposed epithelial hierarchy in the mammary gland.